CORTEX 48 (2012) 389–413

Available online at www.sciencedirect.com

SciVerse ScienceDirect

Journal homepage: www.elsevier.com/locate/cortex

Review

Neuroimaging findings in frontotemporal lobar degeneration spectrum of disorders

Federica Agosta [a,1], Elisa Canu [a,1], Lidia Sarro [a], Giancarlo Comi [b] and Massimo Filippi [a,b,*]

[a] Neuroimaging Research Unit, Institute of Experimental Neurology, Division of Neuroscience, Scientific Institute and University Vita-Salute San Raffaele, Milan, Italy

[b] Department of Neurology, Scientific Institute and University Vita-Salute San Raffaele, Milan, Italy

ARTICLE INFO

Article history:
Received 10 January 2011
Revised 7 March 2011
Accepted 19 April 2011
Action editor Gereon Fink
Published online 1 May 2011

Keywords:
Frontotemporal lobar degeneration (FTLD)
Structural MRI
Diffusion tensor (DT) MRI
Positron emission tomography (PET)
Functional MRI (fMRI)

ABSTRACT

Frontotemporal lobar degeneration (FTLD) is a clinically and pathologically heterogeneous spectrum of disorders. In the last few years, neuroimaging has contributed to the phenotypic characterisation of these patients. Complementary to the clinical and neuropsychological evaluations, structural magnetic resonance imaging (MRI) and functional techniques provide important pieces of information for the diagnosis of FTLD. They also appear to be useful in distinguishing FTLD from patients with Alzheimer's disease (AD). Preliminary studies in pathologically proven cases suggested that distinct patterns of tissue loss could assist in predicting *in vivo* the pathological subtype. Recent years have also witnessed impressive advances in the development of novel imaging approaches. Diffusion tensor MRI and functional MRI have improved our understanding of the pathophysiology of the disease, and this should lead to the identification of additional useful markers of disease progression. This reviews discusses comprehensively the state-of-the-art of neuroimaging in the study of FTLD spectrum of disorders, and attempts to envisage which will be new neuroimaging biomarkers that could serve as surrogate measures of the underlying pathology. This will be central in the design of treatment trials of experimental drugs, which are likely to emerge in the near future, to target the pathological processes associated with this condition.

1. Introduction

Frontotemporal lobar degeneration (FTLD) represents the second most common early onset neurodegenerative dementia (Rabinovici and Miller, 2010). FTLD is a clinically and pathologically heterogeneous spectrum of disorders, which encompasses distinct clinical syndromes: the behavioural variant of frontotemporal dementia (bvFTD), and the language variant (Rabinovici and Miller, 2010). bvFTD presents with marked changes in personality and behaviour (Neary et al., 1998), and, pathologically, is associated with all the three major FTLD pathologies, characterised by abnormal cellular inclusions containing either tau, TAR DNA-binding protein 43 (TDP-43), or fused in sarcoma (FUS) protein (Mackenzie et al.,

* *Corresponding author*. Neuroimaging Research Unit, Institute of Experimental Neurology, Division of Neuroscience, Scientific Institute and University Vita-Salute San Raffaele, Via Olgettina 60, 20132 Milan, Italy.
E-mail address: m.filippi@hsr.it (M. Filippi).

[1] These authors contributed equally to this work.

0010-9452/$ – see front matter © 2011 Elsevier Srl. All rights reserved.
doi:10.1016/j.cortex.2011.04.012

2010). In the language variant, known as primary progressive aphasia (PPA), a prominent, isolated language deficit is the dominant feature during the initial phase of the disease (Mesulam, 2001). Distinct profiles of language impairment define the three clinical phenotypes of PPA (Gorno-Tempini et al., 2011): the non-fluent/agrammatic (for convenience hereafter called as non-fluent), characterised by agrammatism in language production and effortful speech with motor speech deficits; the semantic, characterised by progressive loss of knowledge about words and objects in the context of relatively preserved fluency of speech; and the logopenic, characterised by impaired naming and repetition in the context of spared syntactic and motor speech abilities. The non-fluent variant is most commonly associated with tau pathology (Josephs et al., 2006; Knibb et al., 2006), and the semantic with a TDP-43 proteinopathy (Grossman et al., 2007b; Hodges et al., 2004; Mesulam et al., 2008). Alzheimer's disease (AD) is the most likely underlying pathology of the more controversial logopenic variant, although FTLD with TDP-43 immunoreactive inclusions (FTLD-TDP) changes can also be found (Josephs et al., 2008; Mesulam et al., 2008).

In the last few years, neuroimaging has contributed to the phenotypic characterisation of FTLD. The most commonly used neuroimaging approaches to assess FTLD are structural magnetic resonance imaging (MRI) and functional molecular techniques, i.e., single photon-emission computed tomography (SPECT) and positron emission tomography (PET). Structural MRI showed that each clinical syndrome is associated with a specific pattern of focal atrophy and is routinely used in the diagnostic work up of FTLD. SPECT allows to study cerebral perfusion with compounds such as the [^{99m}Tc]-hexamethylpropyleneamine oxime (HMPAO). PET, most frequently used with [^{18F}]-fluorodeoxyglucose (FDG), provides estimates of cerebral metabolism. Overall, functional neuroimaging techniques offer a window on brain states relative to structural imaging or even in the absence of structural brain abnormalities.

Recent years have also witnessed impressive advances in the development of novel imaging approaches, which, with varying degrees of success, had improved our ability to diagnose and understand the pathophysiology of the disease. Diffusion tensor (DT) MRI allows to measure the random diffusional motion of water molecules and, thus, provides quantitative indices of the structural and orientational features of central nervous system tissues (Pierpaoli et al., 1996). Alterations in the brain microstructure associated with FTLD have the potential to modify water diffusion characteristics, which can be reflected in increased mean diffusivity (MD) and reduced fractional anisotropy (FA) values. The PET ligand [^{11C}]-labelled Pittsburgh compound-B (PIB) binds specifically to fibrillar amyloid β (Aβ) (Klunk et al., 2004). The ability to image Aβ may allow distinction of FTLD from AD with a greater accuracy than that of other structural and functional imaging techniques. Given the costs, limited availability and relative invasiveness of FDG PET, functional MRI (fMRI) is likely to be an useful tool for detecting alterations in brain function that may be present very early in the course of FTLD. In particular, resting state (RS) fMRI has proved to be a new tool for mapping large-scale neural network function and dysfunction in neurodegenerative diseases (Greicius et al., 2004).

This article reviews comprehensively the state-of-the-art of neuroimaging in the study of FTLD spectrum of disorders, and envisages which will be new neuroimaging biomarkers that could improve the *in vivo* detection of the underlying pathology. This will be central in the design of treatment trials of new drugs targeting the pathological processes associated with FTLD, which are likely to emerge in the near future.

2. Structural damage in FTLD syndromes

2.1. *bvFTD*

2.1.1. *The pattern of brain atrophy*

Structural MRI studies showed that bvFTD presents with a combination of frontal and anterior temporal cortical atrophy, usually asymmetrical (Boccardi et al., 2005; Du et al., 2007; Perry et al., 2006; Richards et al., 2009; Rosen et al., 2002; Seeley et al., 2008; Whitwell et al., 2009) (Fig. 1A). Such an atrophy pattern can be readily appreciated on coronal MRI scans. Nevertheless, an apparently normal MRI at visual inspections does not exclude a diagnosis of bvFTD, because tissue loss can be very modest in the early stages of the disease.

The applications of automated quantitative methods, including voxel-based morphometry (VBM) (Boccardi et al., 2005; Rosen et al., 2002; Seeley et al., 2008; Whitwell et al., 2009) and cortical thickness measurement (Du et al., 2007; Richards et al., 2009), revealed that the pattern of atrophy in bvFTD varies significantly across different cohorts (Fig. 2). In the frontal lobe, patients with bvFTD showed atrophy of the bilateral ventromedial frontal and orbitofrontal cortices (Boccardi et al., 2005; Du et al., 2007; Rosen et al., 2002; Seeley et al., 2008), dorsolateral prefrontal cortex (Du et al., 2007; Rosen et al., 2002; Seeley et al., 2008), anterior insula (Boccardi et al., 2005; Rosen et al., 2002; Seeley et al., 2008), anterior cingulate cortex (Boccardi et al., 2005; Rosen et al., 2002; Seeley et al., 2008), and left premotor cortex (Rosen et al., 2002). Atrophy of the temporal lobe includes the amygdala and hippocampus, bilaterally (Barnes et al., 2006; Boccardi et al., 2005; Seeley et al., 2008), as well as the left inferior temporal gyrus (Boccardi et al., 2005).

In some cases, bvFTD presents with a remarkable atrophy of the anterior temporal lobe and a little involvement of the frontal regions (Shimizu et al., 2009; Whitwell et al., 2009). A recent VBM study suggested that bvFTD can be divided into four anatomically different subtypes, two of which are associated with a prominent frontal atrophy (i.e., frontal dominant, and frontotemporal variants) and two other with a prominent temporal lobe atrophy (i.e., temporal dominant, and temporofronto-parietal subtypes) (Whitwell et al., 2009).

Brain damage in bvFTD is not limited to the cortex (Fig. 2); it also involves several subcortical structures, such as the striatum (Boccardi et al., 2005; Garibotto et al., 2009; Seeley et al., 2008), thalamus (Borroni et al., 2007; Garibotto et al., 2009; Seeley et al., 2008), bilaterally, and hypothalamus (Piguet et al., 2010). In addition to frontal and temporal grey matter (GM) atrophy, frontal white matter (WM) loss was also detected in bvFTD patients compared with controls (Cardenas et al., 2007; Seeley et al., 2008). Significant atrophy was also found in the brainstem, including the midbrain and pontine

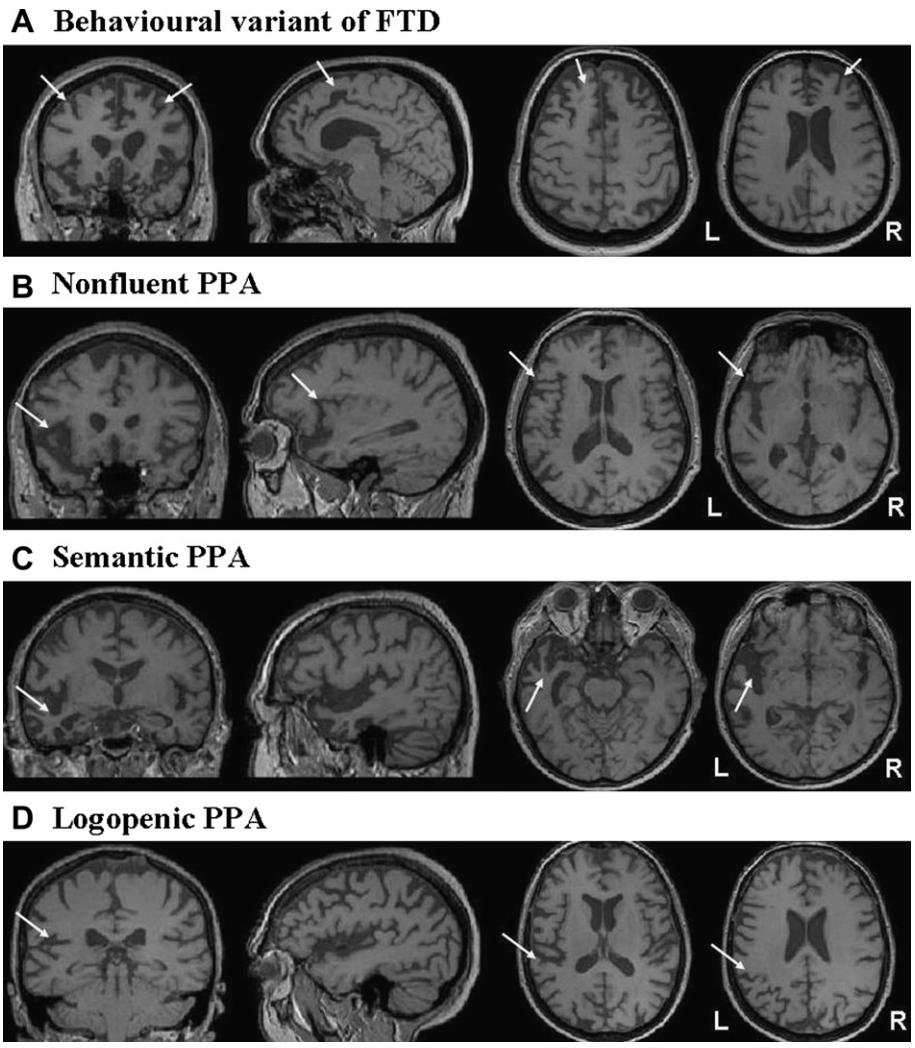

Fig. 1 – T1-weighted MRI scans showing the typical brain atrophy patterns of bvFTD and each PPA variant. (A) A typical bvFTD patient, aged 49 years. The arrows show atrophy of the medial and dorsolateral frontal cortices. (B) A patient with the non-fluent PPA variant, aged 63 years. The arrows show asymmetric left-lateralised atrophy of the insula and inferior frontal gyrus. (C) A semantic PPA patient, aged 66 years. The arrow shows left-lateralised atrophy in the anterior temporal lobe. (D) A logopenic PPA patient, aged 57 years. The arrow shows left-lateralised atrophy in the inferior parietal lobule.

tegmentum (Cardenas et al., 2007; Chao et al., 2007; Seeley et al., 2008).

The pattern of atrophy of bvFTD patients differs from that of other neurodegenerative disorders, including AD (Boccardi et al., 2003; Davatzikos et al., 2008; Du et al., 2007; Richards et al., 2009). Relative to bvFTD, frontal brain regions are generally spared in AD until late stages (Thompson et al., 2007). These findings are supported by studies of autopsy-proven bvFTD and AD patients (Kloppel et al., 2008; Likeman et al., 2005; Rabinovici et al., 2007b; Vemuri et al., 2010). Compared with AD patients, autopsy-proven bvFTD patients had an atrophy pattern involving the anterior cingulate, frontal insula, subcallosal gyrus, and striatum, bilaterally, whereas AD patients showed a greater atrophy in the posterior parietal and occipital cortices (Rabinovici et al., 2007b). In a study investigating the diagnostic accuracy of visual inspection of MRI scans in patients with pathologically confirmed diagnosis, atrophy of the anterior, inferior, and lateral temporal lobes was associated with the highest sensitivity (≥90%) for discriminating bvFTD from AD patients, and anterior greater than posterior gradient and hemispheric asymmetry of atrophy were each at least 85% specific for bvFTD versus AD (Likeman et al., 2005). Supervised machine learning techniques applied to standard T1-weighted MRI scans of autopsy-proven FTLD (including bvFTD patients) and AD cases performed well in distinguishing the two forms of dementia (Kloppel et al., 2008; Vemuri et al., 2010).

Patterns of brain atrophy might be predictive of the underlying pathological process in bvFTD (Table 1), with bilateral dorsolateral prefrontal atrophy and milder temporal atrophy being suggestive of Pick's disease (PiD), and asymmetric left and right temporal lobe atrophy being associated with FTLD with ubiquitin-positive pathology (FTLD-U) and FTLD with tau-positive inclusions (FTLD-tau), respectively (Whitwell et al., 2005). A similar pattern of bilateral fronto-temporal atrophy was found in FTLD-tau and FTLD-TDP cases

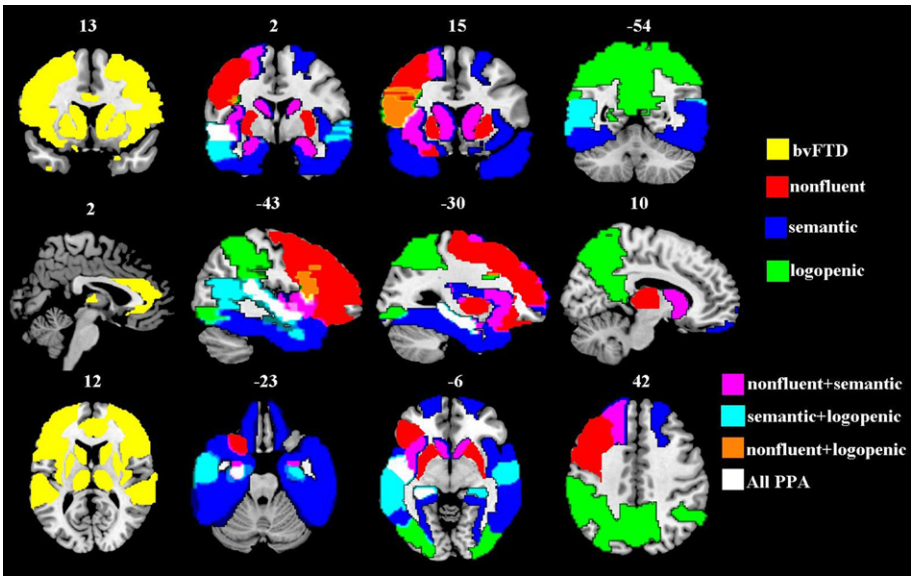

Fig. 2 – This illustrative figure shows the patterns of GM atrophy in patients with bvFTD and each PPA variant, as derived from available literature. Regions of GM atrophy are overlaid on the sagittal, coronal and axial slices of the Montreal Neurological Institute template.

in other studies (Kim et al., 2007; Pereira et al., 2009; Whitwell et al., 2004b), with a more severe striatal atrophy observed in FTLD-tau cases in one series (Kim et al., 2007). Two recent studies revealed distinct patterns of atrophy among the pathological subtypes of FTLD-TDP (Rohrer et al., 2010a; Whitwell et al., 2010). In the first study (Rohrer et al., 2010a), bvFTD patients with type 2 or type 3 pathology according to Sampathu nomenclature (Sampathu et al., 2006) showed a relatively symmetric atrophy of the medial temporal lobe, medial prefrontal, and orbitofrontal/insular cortices (type 2) or asymmetric atrophy involving more dorsal areas including frontal, temporal, and inferior parietal cortices, as well as the striatum and thalamus, bilaterally (type 3). In the second study (Whitwell et al., 2010), bvFTD patients with type 1 or type 3 pathology according to Mackenzie et al. (2006) (which correspond to Sampathu type 3 or type 2, respectively) experienced frontotemporal and parietal atrophy or predominantly posterior frontal atrophy, respectively (Fig. 3). However, within the FTLD-TDP Mackenzie type 1 group, patients with a progranulin mutation had more lateral temporal lobe atrophy than those without, and patients with motor neuron degeneration had a similar pattern of atrophy, regardless the type of FTLD-TDP pathology (Whitwell et al., 2010). Marked atrophy of the caudate nucleus in bvFTD patients might be predictive of FTLD with fused in sarcoma protein inclusions (FTLD-FUS) pathology (Josephs et al., 2010b; Rohrer et al., 2010b; Seelaar et al., 2010). Taken together, the results of these studies suggest that the patterns of atrophy may contribute to the *in vivo* prediction of the underlying FTLD pathology. They also demonstrated that FTLD-TDP is not an anatomically homogeneous entity, and patterns of atrophy in this condition differ in case of progranulin mutation and motor neuron disease occurs. However, caution should be exerted when interpreting these findings because the samples of patients studied were small. As a consequence, further work is needed to better understand similarities and diversities among the FTLD spectrum of pathology.

Summary

- bvFTD presents with a combination of frontal, anterior temporal cortical and subcortical atrophy.
- Anterior greater than posterior gradient and hemispheric asymmetry of involvement provide the highest specificity for discriminating bvFTD from AD.
- Patterns of brain atrophy are likely to be associated with the different pathological substrates of bvFTD.

2.1.2. *Atrophy progression*

In line with pathological findings, cross-sectional (Seeley et al., 2008) and longitudinal (Brambati et al., 2007; Chan et al., 2001a; Whitwell et al., 2004a) volumetric studies showed that very mild bvFTD targets a specific subset of frontal and insular regions, while more advanced disease affects WM and posterior GM structures.

In a cross-sectional VBM study, patients with bvFTD were stratified based on their clinical dementia rating (CDR) score and atrophy patterns were determined in the different clinical stages (Seeley et al., 2008). Patients with mild dementia severity (CDR = .5) showed circumscribed GM atrophy in a network of anterior brain regions, including paralimbic (anterior cingulate cortex, frontoinsula, and lateral orbitofrontal cortex), frontal neocortical (dorsolateral, rostromedial, and frontal polar), limbic (hippocampus), and subcortical (ventral striatum and dorsomedial thalamus) areas, as well as the precentral gyrus, with a predominant involvement of the right hemisphere. At CDR = .5 WM loss was minimal, with only small subfrontal and basal pontine foci detected. In patients with CDR score of 1, GM atrophy was more extensive and bilateral, involving most of the medial frontal surface, dorsolateral frontal regions and

Table 1 – Patterns of brain atrophy in patients with different frontotemporal lobar degeneration pathology.

	Pathology	bvFTD	Non-fluent[a]	Semantic	Logopenic	Atrophy pattern
Whitwell et al. (2004b)	FTLD-tau[b]					Atrophy of frontal and temporal cortices (right > left).
	FTLD-U[b]					Atrophy of frontal and temporal cortices (right > left).
Whitwell et al. (2005)	FTLD-tau	5/16 (tau exon 10 + 16)				Asymmetric (right > left) anterior and medial temporal lobe and orbitofrontal cortex atrophy.
		5/16 (PiD)	1/1 (PiD)	1/4 (PiD)		Severe dorsolateral bifrontal atrophy, with milder atrophy of the temporal lobes.
	FTLD-U	6/16		3/4		Asymmetric (left > right) frontal and temporal atrophy.
Kim et al. (2007)	FTLD-tau	5/10		1/3		Frontal, anterior temporal and striatal atrophy. Striatal atrophy more severe than in FTLD-U cases.
	FTLD-U	5/10	1/1	2/3		Frontal, anterior temporal and striatal atrophy.
Grossman et al. (2007a)	FTLD-tau		5/9			Cortical atrophy in the frontal and parietal regions, more prominent in the right hemisphere.
	FTLD-U		2/9	3/4		Cortical atrophy in the frontal and temporal regions.
	Other		2/9 (AD)	1/4 (AD)		Atrophy of the bilateral parietal and temporal areas, including the hippocampus.
Josephs et al. (2008)	FTLD-U			5/10		Left-sided temporal lobe atrophy, including the amygdala, hippocampus, inferior and middle temporal gyri, and fusiform gyrus.
	Other			5/10 (AD)		Left-sided temporoparietal lobe atrophy, with sparing of the medial and anterior temporal pole.
Rohrer et al. (2009)	FTLD-tau		4/4 (2 CBD; 2 PiD)			Significant thinning in the left insula.
	FTLD-U			11/11		Asymmetric (left > right) thinning of the temporal cortices.
Pereira et al. (2009)	FTLD-tau	1/4	2/3	3/11		Bilateral mesial frontal and insular cortices atrophy
	FTLD-U	3/4	1/3	5/11		Bilateral mesial frontal and insular cortices atrophy
	Other			3/11 (AD)		Severe left hippocampal atrophy, and absence of the knife-edge anterior temporal atrophy and of the severe thinning of the temporal lobe in the regions of the collateral sulcus and fusiform gyrus seen in other semantic groups.
Hu et al. (2010)	FTLD-tau		3/3 (2 CBD, 1 PSP)			Dorsolateral prefrontal and insular atrophy.
	FTLD-U				2/4 FTLD-TDP	Peri-sylvian atrophy.
	Other				2/4 (AD)	Posterior-superior temporal atrophy
Rohrer et al. (2010a)[c]	FTLD-U	4/4 FTLD-TDP (2: Sampathu type 2; 2: Sampathu type 3)	3/3 FTLD-TDP (Sampathu type 3)	9/9 FTLD-TDP (Sampathu type 1)		Sampathu type 1: asymmetric anterior temporal atrophy, orbitofrontal and insular atrophy. Sampathu type 2: symmetric atrophy of the medial temporal, medial prefrontal, and orbitofrontal-insular cortices. Sampathu type 3: asymmetric atrophy involving more dorsal areas including frontal, temporal, and inferior parietal cortices, striatum, and thalamus.

(*continued on next page*)

Table 1 – (*continued*)

	Pathology	bvFTD	Non-fluent[a]	Semantic	Logopenic	Atrophy pattern
Whitwell et al. (2010) [c]	FTLD-U	18/18 FTLD-TDP (13: Mackenzie type 1; 5: Mackenzie type 3)	1/1 FTLD-TDP (Mackenzie type 1)	9/9 FTLD-TDP (Mackenzie type 2)		Mackenzie type 1: frontotemporal and parietal atrophy. Mackenzie type 2: predominantly anterior temporal lobe atrophy. Mackenzie type 3: predominantly posterior frontal atrophy.
Josephs et al. (2010b)	Other	3/3 (FTLD-FUS)				Greater caudate nucleus atrophy compared with FTLD-tau and FTLD-TDP cases.
Rohrer et al. (2010b)	Other	5/5 (FTLD-FUS)				Atrophy of frontoinsular and anterior cingulate cortices and caudate nucleus.

a Includes patients with non-fluent aphasia before the recognition of logopenic variant.
b The study included 13 bvFTD, one non-fluent, and three semantic patients; nine patients had a tau pathology (four cases with FTLD-17, and five cases with sporadic PiD), while eight patients had an FTDL-U pathology; however, the phenotypic distribution among different pathologic groups is not reported.
c These studies used different nomenclatures of the TDP-43 subtypes, i.e., Sampathu (Sampathu et al., 2006) versus Mackenzie (Mackenzie et al., 2006). The correspondence between the two schemes is as follows: Sampathu type 1 = Mackenzie type 2; Sampathu type 2 = Mackenzie type 3; and Sampathu type 3 = Mackenzie type 1.

striatal-thalamic structures. WM loss involved the subfrontal, parahippocampal, midcallosal regions and cerebral peduncles. In patients with CDR scores of 2 or 3, which indicate moderate and severe dementia stages respectively, the GM of the frontal lobe was markedly involved, as well as the posterior insula, posterior hippocampus, and parietal lobes, bilaterally. In these stages, WM loss affected the entire corpus callosum, as well as several subcortical regions (including parahippocampal areas and parietal lobes).

Increased rates of whole brain (WB) atrophy have been observed in bvFTD patients compared with age-matched healthy controls (Table 2) (Chan et al., 2001a; Gordon et al., 2010; Knopman et al., 2009; Whitwell et al., 2008, 2007a). Using the boundary-shift integral method to quantify changes over time of WB volume and ventricular enlargement (VE) (Chan et al., 2001a; Gordon et al., 2010; Knopman et al., 2009), it was shown that the annual rate of WB volume loss varies from 1.4% to 3.7%, while the annual VE was found to be around 6 ml/year. The topographical distribution of progressive brain atrophy in bvFTD patients has been assessed by a few longitudinal studies (Brambati et al., 2007; Chan et al., 2001a; Whitwell et al., 2004a). A first regional analysis study found that progression of atrophy occurs predominantly in the anterior brain quadrants including the frontal lobes and the temporal poles (Chan et al., 2001a). Comparing two serial structural MRI scans using a fluid registration technique, a significant volume loss compared with controls was observed in the posterior cingulate cortex from 10 bvFTD patients, thus suggesting that the medial parietal lobes may be affected later in the course of the disease (Whitwell et al., 2004a). More recently, a WB analysis of bvFTD using tensor-based morphometry found that the anterior cingulate/paracingulate gyri showed GM contraction over 1 year in bvFTD (Brambati et al., 2007), confirming the vulnerability of limbic and paralimbic regions in this disease. When a region of interest (ROI)-based approach was applied, the left ventromedial frontal cortex, right medial superior frontal gyrus, anterior insulae and left amygdala/hippocampus showed additional significant longitudinal volume losses (Brambati et al., 2007).

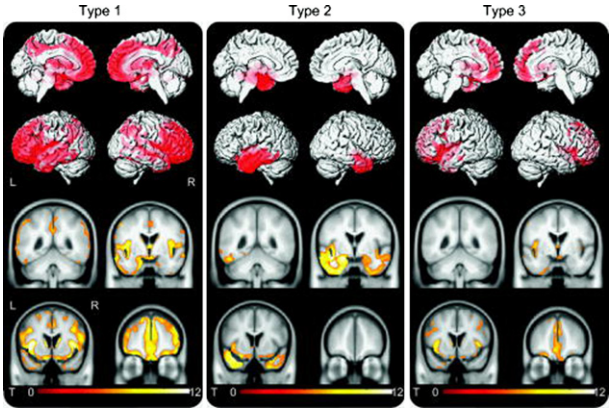

Fig. 3 – Patterns of GM atrophy in FTLD-TDP types 1, 2, and 3 compared with age-matched healthy controls. From Whitwell et al. (2010) [permission requested].

Compared to AD, the progression of atrophy in bvFTD patients is faster (Chan et al., 2001a; Whitwell et al., 2008). Chan et al. (2001a) showed that bvFTD and AD are associated with different rates of atrophy [mean annual losses 3.7% (range: .3–8.0%) and 2.4% (range: .5–4.7%), respectively]. Similarly, the annual rate of WB volume loss in FTLD-U subjects, including both bvFTD and PPA patients, was significantly higher than the rate observed in AD subjects (Whitwell et al., 2008). The results of a regional analysis of atrophy showed that there were differences between bvFTD and AD patients in the rates of tissue loss of both anterior quadrants of the brain, but not in the posterior quadrants (Chan et al., 2001a). A more recent study showed that, although atrophy rates were significantly higher in the cingulate and hippocampi in both bvFTD and AD compared with controls, there was evidence of a subregional difference in trends of atrophy in the cingulate between the disease groups (more anterior in bvFTD and more posterior in AD) (Barnes et al., 2007).

Table 2 – Annual rates of change of MRI measures in longitudinal studies in patients with the bvFTD and PPA variants compared with healthy controls and patients with AD.

Study		Controls	bvFTD	Non-fluent	Semantic	Logopenic	FTLD-U[a]	AD
Chan et al. (2001a)	N	27	17		13[b]			54
	Mean WB volume loss/y [standard deviation (SD)] [%]	.47 (.40)	3.7 (2.5)		2.5 (1.0)			2.37 (1.03)
Whitwell et al. (2007a)	N	25					12	12
	Median WB volume loss/y (range) [%][c]	−.3 (1.2, −.8)					−1.7 (−.9, −5.6)	−1.1 (.4, −3.8)
	Median VE/y (range) [%][c]	3.1 (−2.8, 7.5)					9.6 (8.6, 33.7)	8.3 (2.4, 16.0)
Whitwell et al. (2008)	N						9	9
	Mean WB volume loss/y [95% confidence interval (CI)] [ml/y]						23 (15–31)	10 (2–18)
	Mean VE/y (95% CI) [ml/y]						1.66 (.5–2.81)	.44 (−.38–1.26)
Rohrer et al. (2008)	N				21		8	
	Mean WB volume loss/y [ml/y]	4.4 (4.1)			27.4 (16.0)		21.6 (6.1)	
	Mean VE/y (SD) [ml/y]	.7 (1.0)			6.9 (3.8)		4.5 (1.3)	
Knopman et al. (2009)	N		34	17	16	9		
	Mean WB volume loss/y (SD) [%]		1.60 (1.11)	1.61 (.89)	1.66 (1.04)	2.08 (1.00)		
	Mean VE/y (SD) [ml/y]		5.94 (4.40)	6.33 (4.47)	7.42 (3.95)	4.79 (1.89)		
Gordon et al. (2010)	N	24	11	10	11			
	Mean WB volume loss/y (SD) [%]	.1 (.5)	1.4 (1.5)	2.9 (.9)	2.6 (1.6)			
	Mean VE/y (SD) [ml/y]	.5 (1.1)	5.5 (6.7)	5.6 (3.8)	7.1 (4.9)			

a FTLD-U subjects had a clinical diagnosis of bvFTD or PPA.
b One patient had a clinical picture suggestive of non-fluent PPA.
c Data are shown as median (range). Negative rates represent a decrease in volume over time, whereas positive rates represent an increase in volume.

Summary

- Very mild bvFTD targets a specific subset of frontal and insular regions, while more advanced disease affects WM and posterior GM structures.
- Compared to AD, the progression of atrophy in bvFTD patients is faster, with the most striking differences in anterior brain regions.

2.1.3. *Intrinsic tissue abnormalities*

A recent DT MRI study of bvFTD patients (Whitwell et al., 2011) found a pattern of GM increased MD that mirrors closely that of GM loss, including the frontal and anterior temporal lobes, insula, and caudate nucleus, bilaterally. Increased MD was also found in the parietal and occipital GM (Whitwell et al., 2011).

In a single, pathology-proven bvFTD case, ROI-based DT MRI detected decreased FA values in WM frontal regions, where histopathology revealed a typical frontal lobe degeneration of non-AD type (Larsson et al., 2004). Using a ROI-based approach *in vivo*, a recent bvFTD study found DT MRI abnormalities in WM tracts located in the frontal lobes, such as the anterior cingulum, genu of the corpus callosum, and anterior superior longitudinal fasciculus (SLF), and in those tracts passing through the temporal lobes, such as the uncinate and inferior longitudinal fasciculus (ILF) (Whitwell et al., 2011). Voxel-based DT MRI studies in bvFTD patients found FA reduction in fronto-parietal regions, which are likely to represent the SLF (Borroni et al., 2007), and in frontal and temporal WM regions including the anterior corpus callosum, anterior cingulum, and uncinate, bilaterally (Zhang et al., 2009). Such findings were confirmed by a DT MRI tractography study, which disclosed a significant FA decrease in all major association WM tracts (ILF, uncinate, and SLF) and in the genu of the corpus callosum, as well as a sparing of corticospinal tracts and splenium of the corpus callosum (Matsuo et al., 2008). Two studies identified diffusivity changes also in more posterior WM regions, such as those containing the posterior SLF and the posterior cingulum (Whitwell et al., 2011; Zhang et al., 2009).

DT MRI may improve the diagnostic differentiation between bvFTD and AD. When compared with AD, bvFTD was associated with greater reductions of FA in frontal regions, whereas no regions in AD showed greater DT MRI changes compared to bvFTD (Fig. 4) (Zhang et al., 2009). One recent study combined cortical thickness measurement and DT MRI to compare 25 FTLD (13 bvFTD, seven non-fluent, five semantic) and 24 AD patients, with autopsy- or cerebrospinal fluid (CSF)-confirmed disease (Avants et al., 2010). The direct comparison of the two groups showed a significantly greater atrophy in inferior frontal, medial frontal and prefrontal cortical regions, and a reduced FA of the genu of the corpus callosum, left inferior fronto-occipital fasciculus (IFOF), cingulum, uncinate and bilateral corona radiata in FTLD cases relative to AD (Avants et al., 2010). Conversely, AD patients showed no areas of significant reduction in cortical thickness or WM integrity relative to FTLD

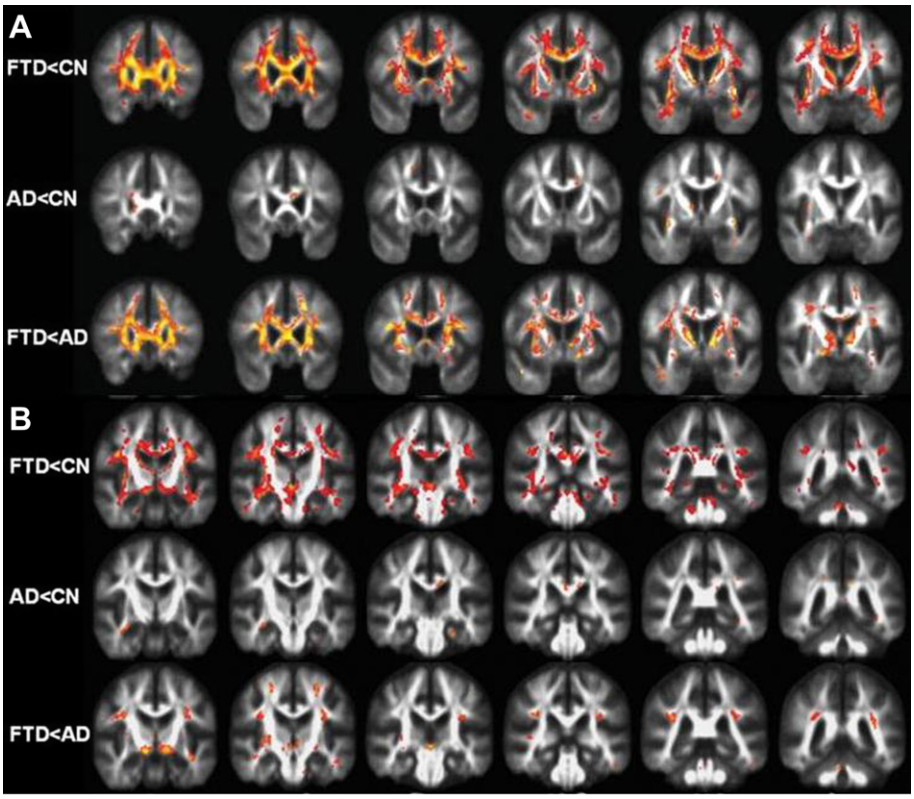

Fig. 4 – DT MRI abnormalities in patients with bvFTD compared with those from patients with AD in the anterior (A) and posterior (B) brain regions. (A) The first row [FTD < cognitively normal (CN)] shows FA reductions in bvFTD patients relative to CN individuals involving the anterior frontal and temporal brain. The second row (AD < CN) shows the regional FA reductions in AD patients relative to CN individuals involving only a few regions in left anterior cingulum and bilateral uncinate fasciculus. The third row (FTD < AD) shows FA reductions in bvFTD relative to AD patients indicating that bvFTD patients had significantly lower FA values in several regions located in the bilateral frontal lobes, including the anterior corpus callosum, bilateral anterior cingulum, uncinate fasciculus and anterior limb of internal capsule. (B) The first row (FTD < CN) shows FA reductions in bvFTD patients relative to CN individuals involving the posterior brain regions. BvFTD patients compared to CN individuals experienced widely distributed changes involving the posterior brain (but not as severe as in the anterior brain) including posterior corpus callosum, bilateral posterior cingulum, descending cingulum, as well as fibres in the SLF. The second row (AD < CN) shows the regional FA reductions in AD patients relative to CN individuals involving a few regions located in the left posterior cingulum and left descending cingulum. The third row (FTD < AD) shows FA reductions in bvFTD relative to AD patients indicating that bvFTD had significantly lower FA values in regions of the bilateral SLF and inferior part of the thalamus. The areas with significantly decreased FA values are marked in warm colours with p-False Discovery rate threshold = .05. Modified from Zhang et al. (2009) with permission.

patients (Avants et al., 2010). These studies suggest that WM injury is likely to be more prominent in bvFTD than in AD.

Summary

- In bvFTD, DT MRI abnormalities involve preferentially WM tracts located in the frontal lobes and those passing through the temporal lobes. However, diffusivity changes are also identified in more posterior WM regions.
- Compared with AD, bvFTD is associated with a more prominent frontal WM damage, whereas no regions in AD showed more severe DT MRI abnormalities compared to bvFTD.

2.1.4. *Clinical correlates*

Several previous studies have reported an association between regional volume loss in the frontal cortex and cognitive and behavioural symptoms of bvFTD. Using VBM, aberrant behaviours in bvFTD, as measured by the neuropsychiatric inventory (NPI), were found to correlate with GM volume loss in the dorso-mesial frontal lobe/paracingulate region, which was more prominent on the right side (Williams et al., 2005). Behavioural dysfunction in a large group of 148 dementia patients, including 32 patients with bvFTD, was correlated with atrophy in several brain regions of the right hemisphere including the ventral portion of the anterior cingulate cortex and the adjacent ventromedial superior frontal gyrus, ventromedial prefrontal cortex, orbitofrontal cortex, lateral middle frontal gyrus and anterior insula (Rosen et al., 2005). In addition, three regions of the medial frontal cortex showed unique associations with specific behaviours: apathy correlated with tissue loss in the ventromedial superior frontal gyrus, disinhibition with tissue loss in the

subgenual cingulate gyrus, and aberrant motor behaviour with tissue loss in the dorsal anterior cingulate cortex and premotor cortex (Rosen et al., 2005). This observation has been partially corroborated by another study, which indicated that partially distinct areas of cortical atrophy are associated with apathy and disinhibition, including the dorsal anterior cingulate cortex and dorsolateral prefrontal cortex in apathetic patients, and the medial orbital frontal cortex in disinhibited patients (Massimo et al., 2009).

Many behavioural features in bvFTD have been also associated with right temporal lobe atrophy (Zamboni et al., 2008). A VBM study including 48 bvFTD patients and 14 subjects with an aphasic variant, showed that the severity of apathy correlated with atrophy in the right dorsolateral prefrontal cortex, while the severity of disinhibition correlated with atrophy in the right nucleus accumbens, right superior temporal sulcus, and right mediotemporal limbic structures (Zamboni et al., 2008). GM volumes of the right subcortical and deep cortical structures (i.e., caudate, putamen, and amygdala) have been found to correlate negatively with behavioural symptoms in bvFTD as measured by the frontal behaviour inventory (FBI) (Garibotto et al., 2009).

In bvFTD patients, neuroanatomical correlates of different abnormalities of eating behaviour (pathological sweet tooth and increased food consumption, or hyperphagia) were also identified (Piguet et al., 2010; Whitwell et al., 2007b; Woolley et al., 2007). The development of pathological sweet tooth was associated with GM loss in a distributed brain network including bilateral posterolateral orbitofrontal cortex and right anterior insula (Whitwell et al., 2007b). Hyperphagia was associated with more focal GM loss in anterolateral orbitofrontal cortex, bilaterally, in one study (Whitwell et al., 2007b), and atrophy of the right ventral insula, striatum, and orbitofrontal cortex in another one (Woolley et al., 2007). Patients with severe feeding disturbances, such as increased appetite, preference for sweet foods, and increased tendency to eat the same foods, exhibited significant atrophy of the posterior hypothalamus (Piguet et al., 2010).

Serial MRI studies showed that the annualised percent changes of WB volume at 1 year is associated with decline in Mini Mental State Examination (MMSE) (Gordon et al., 2010) and CDR-sum of boxes (SB) (Gordon et al., 2010; Knopman et al., 2009) scores measured in bvFTD patients. In addition, in these patients, FA values of the right SLF were found to correlate negatively with the Trail Making Test-B score, which assesses executive functions, and scores of those items of the FBI investigating lack of flexibility, planning deficits, impulsivity or poor judgement, and utilisation behaviour (Borroni et al., 2007). An association was also found between FA values of the left uncinate and MMSE and CDR scores (Matsuo et al., 2008).

Summary

- Partially distinct areas of the medial frontal cortex show unique associations with specific behaviours in bvFTD.
- Many behavioural features in bvFTD are associated with right temporal lobe atrophy.
- Neuroanatomical correlates of different abnormalities of eating behaviour in bvFTD patients are well defined and include GM loss of bilateral orbitofrontal cortex, right insula, and posterior hypothalamus.

2.2. PPA

2.2.1. The pattern of brain atrophy

2.2.1.1. The non-fluent variant. The non-fluent variant is associated with a characteristic pattern of left anterior peri-sylvian atrophy involving inferior, opercular and insular portions of the frontal lobe (Figs. 1B and 2) (Gorno-Tempini et al., 2004a). Motor and premotor regions and Broca's area are also involved (Gorno-Tempini et al., 2004a). A recent study showed that non-fluent patients relative to controls experience the most significant cortical thinning in the left superior temporal sulcus (reduced by 14%), superior temporal lobe (10%), transverse temporal gyrus (9%), left inferior frontal lobe (9%), and superior frontal lobe (9%) (Rohrer et al., 2009). Cortical thinning was also detected in the left insula (Rohrer et al., 2009). Compared with semantic patients, areas that were significantly thinner in non-fluent patients were mainly located in the left hemisphere and included the inferior and superior frontal gyri, precentral gyrus, transverse temporal gyrus, and superior and inferior parietal gyri (Rohrer et al., 2009). In the right hemisphere, some frontal and parietal regions were more atrophied in non-fluent than in semantic patients (Rohrer et al., 2009).

In non-fluent patients, atrophy of the basal ganglia (Garibotto et al., 2009; Gorno-Tempini et al., 2004a), thalamus (Garibotto et al., 2009), and amygdala, bilaterally (Garibotto et al., 2009) was also observed (Fig. 2). Compared with controls, non-fluent patients also had atrophy of the left hippocampus (van de Pol et al., 2006b); however, it was less severe than that in AD patients (van de Pol et al., 2006b). A study investigating WM volume loss in non-fluent patients found a severe involvement of a frontal region, which is likely to harbour part of the SLF (Rohrer et al., 2010d).

Volumetric studies in pathologically confirmed non-fluent cases included only small numbers of subjects (Table 1), but showed findings supporting those reported by clinical cohort studies (Grossman et al., 2007a; Hu et al., 2010; Kim et al., 2007; Pereira et al., 2009; Rohrer et al., 2010a, 2009; Whitwell et al., 2010, 2005, 2004b). Inferior frontal and superior temporal cortical thinning was seen in non-fluent patients with tau-positive disease (Rohrer et al., 2009). Grossman et al. (2007a) detected cortical atrophy in the frontal and parietal regions, more prominent in the right side, in five non-fluent patients with FTLD-tau pathology, and a pattern of frontotemporal atrophy in two non-fluent patients with FTLD-U. Three non-fluent patients with FTLD-TDP Sampathu type 3 pathology showed a dorsal pattern of asymmetric atrophy affecting the frontal, temporal, and insular lobes, as well as the anterior cingulate and parietal areas (Rohrer et al., 2010a). Whitwell et al. (2010) described one non-fluent case with FTLD-TDP Mackenzie type 1 pathology, showing a pattern of frontotemporal and parietal atrophy. In a recent study (Hu et al., 2010), 6 of 19 patients with non-fluent PPA (32%) had CSF findings consistent with AD and showed significant posterior–superior temporal atrophy, while non-fluent patients with FTLD pathology [i.e., corticobasal degeneration (CBD) or progressive supranuclear palsy (PSP) pathology] had dorsolateral prefrontal and insular atrophy (Fig. 5A).

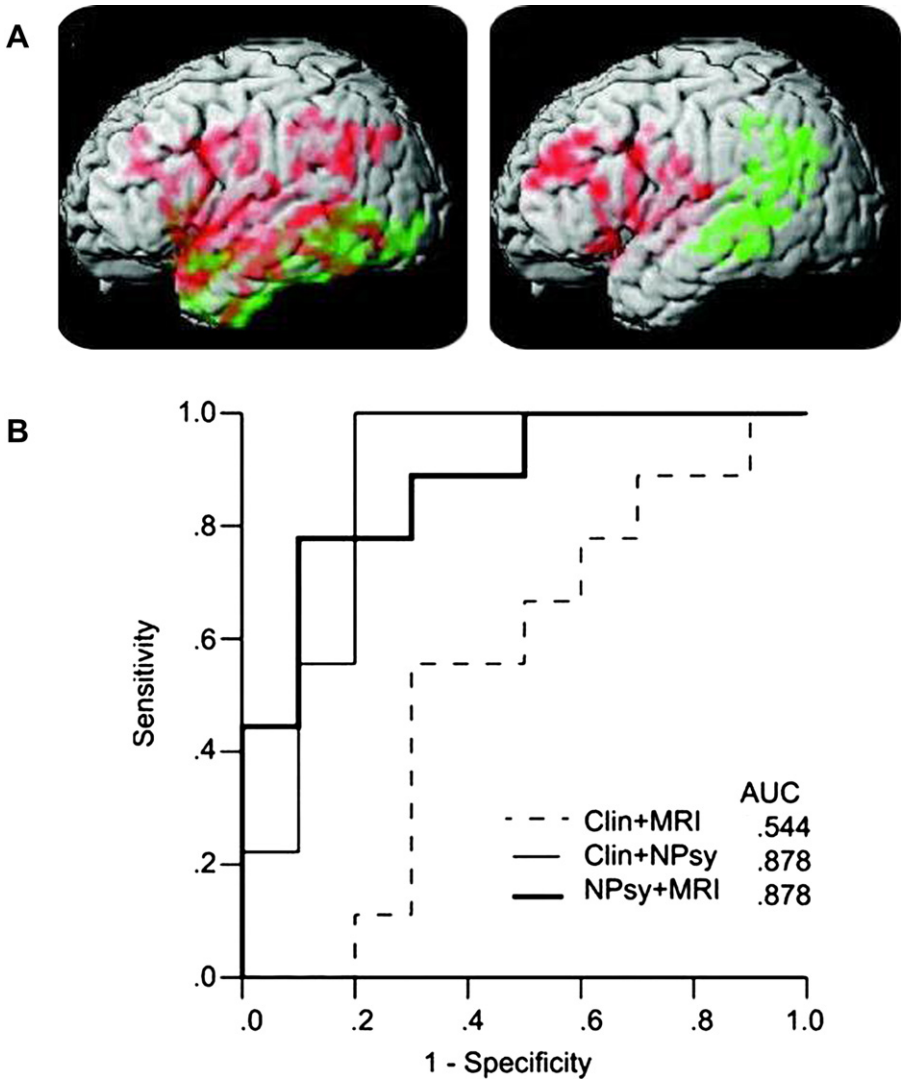

Fig. 5 – (A) Patients with the logopenic variant (left) and non-fluent variant (right) have a frontotemporal atrophy (red) when their CSF biomarkers or autopsy results are consistent with FTLD, and a temporal-parietal atrophy (green) when their CSF biomarkers or autopsy results are consistent with AD. A statistical height threshold for these analyses was set at $p < .005$ and only clusters comprised of 100 or more adjacent voxels that survived a peak voxel significance of $p < .05$ (corrected for family wise error) were accepted. (B) Predictive value of combining clinical features, neuropsychological analysis, and MRI patterns of atrophy for the distinction between FTLD and AD. Abbreviations: AUC = area under the curve; Clin = clinical characterisation; MRI = volumetric MRI analysis; NPsy = neuropsychological analysis. From Hu et al. (2010) [permission requested].

2.2.1.2. The semantic variant. Semantic PPA is associated with left anterior temporal atrophy affecting the lateral and ventral temporal surfaces, as well as the anterior hippocampus and amygdala (Fig. 1C). Regional volumetric studies (Fig. 2) showed a pattern of temporal atrophy including the temporal pole (Boxer et al., 2003; Galton et al., 2001; Gorno-Tempini et al., 2004a; Hodges et al., 1992; Mummery et al., 2000, 1999), amygdala (Barnes et al., 2006; Boxer et al., 2003; Chan et al., 2001b; Galton et al., 2001; Garibotto et al., 2009; Gorno-Tempini et al., 2004a; Rosen et al., 2002), hippocampus (Boxer et al., 2003; Chan et al., 2001b; Galton et al., 2001; Gorno-Tempini et al., 2004a; Rosen et al., 2002; van de Pol et al., 2006a), anterior inferior, middle and superior temporal gyri (Gorno-Tempini et al., 2004a; Hodges et al., 1992; Mummery et al., 1999), and anterior fusiform gyrus (Chan et al., 2001b; Galton et al., 2001; Gorno-Tempini et al., 2004a; Hodges et al., 1992; Mummery et al., 1999), predominantly in the left hemisphere. An involvement of the ventromedial frontal cortex (Gorno-Tempini et al., 2004a; Rosen et al., 2002), caudate nucleus (Gorno-Tempini et al., 2004a), and left posterior insula (Gorno-Tempini et al., 2004a) was also shown. In a recent cortical thickness study (Rohrer et al., 2009), semantic patients experienced the greatest thinning compared with healthy controls in the left anterior and inferior temporal lobes, including the temporal pole (reduced by 51% relative to controls), entorhinal cortex (46%),

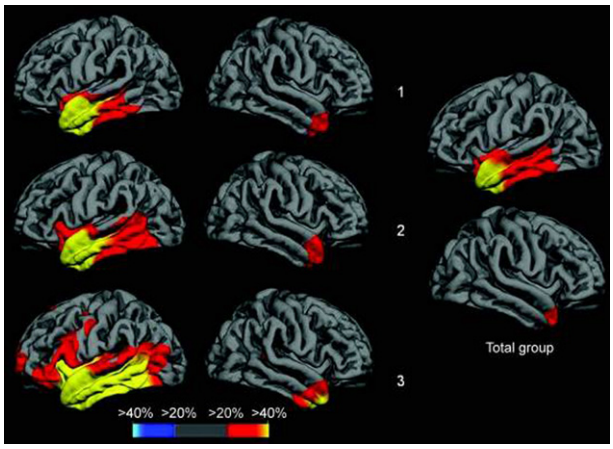

Fig. 6 – Cortical thinning in patients with semantic PPA variant compared with healthy controls. (Left) Percentage cortical thickness differences compared with controls are shown in semantic patients classified based on their naming test scores, i.e., group 1 was the least anomic, and group 3 the most anomic. (Right) Pattern of cortical thinning in all semantic patients compared with controls. Only lateral views are shown. Coloured bar represents percentage thickness difference. From Rohrer et al. (2009) [permission requested].

parahippocampal (30%), fusiform (27%), and inferior temporal (26%) gyri (Fig. 6). In the right hemisphere, a similar but less extensive pattern of cortical thinning was seen (Fig. 6). Compared with non-fluent patients, areas that were significantly thinner in semantic patients were the temporal pole, parahippocampal, entorhinal, fusiform, inferior temporal, middle temporal, and superior temporal gyri in the left hemisphere, and corresponding areas (except for the superior temporal gyrus) in the right temporal lobe (Rohrer et al., 2009).

Patients with the semantic variant also experience temporal WM atrophy (Chao et al., 2007; Rohrer et al., 2010d), which is predominant in the left temporal lobe and includes areas likely to represent the fornix, ILF, and uncinate fasciculus (Rohrer et al., 2010d). Adding temporal WM volume to temporal GM volume significantly improves the discrimination between semantic and bvFTD patients (Chao et al., 2007).

Semantic patients have a left hippocampal atrophy more marked than that seen in AD patients (Boxer et al., 2003; Chan et al., 2001b; Galton et al., 2001; van de Pol et al., 2006a). In semantic PPA, however, the hippocampal atrophy is predominantly located anteriorly, with a relative preservation of the posterior hippocampal regions (Boxer et al., 2003; Chan et al., 2001b). A VBM study, comparing semantic and AD patients (Boxer et al., 2003), found that semantic patients had a greater atrophy of the anterior hippocampus and amygdale, bilaterally, left anterior temporal lobe, and left dorsomedial thalamus compared to both healthy controls and AD patients. On the contrary, compared to semantic patients, those with AD showed a greater atrophy of the left parietal cortex, posterior cingulate cortex, and precuneus, bilaterally (Boxer et al., 2003).

A prominent left frontal and anterior temporal atrophy is seen in patients with semantic PPA who have FTLD-U pathology at autopsy (Grossman et al., 2007a; Josephs et al., 2008; Kim et al., 2007; Rohrer et al., 2009; Whitwell et al., 2005) (Table 1). One recent study (Pereira et al., 2009) showed similar patterns of atrophy in the FTLD-TDP and FTLD-tau semantic patients, as well as a qualitatively different pattern in those with AD. These latter patients mostly has hippocampal involvement, and a lack of the knife-edge anterior temporal atrophy, as well as a less severe thinning of the temporal lobe in the regions of the collateral sulcus and fusiform gyrus. Nine semantic patients with FTLD-TDP Sampathu type 1 pathology showed an asymmetric anterior temporal lobe atrophy (either left- or right-predominant) with additional involvement of the orbitofrontal lobes and insulae (Rohrer et al., 2010a). In another series, nine semantic patients with FTLD-TDP Mackenzie type 2 pathology showed a predominantly anterior temporal lobe atrophy (Whitwell et al., 2010).

2.2.1.3. The logopenic variant. In the logopenic variant, the pattern of atrophy primarily affects the left temporoparietal junction, including the left posterior–superior and middle temporal gyri, as well as the inferior parietal lobule (Figs. 1D and 2) (Gorno-Tempini et al., 2008, 2004a; Migliaccio et al., 2009; Rohrer et al., 2010d). The involvement of the left medial temporal lobe is reported less consistently (Gorno-Tempini et al., 2008). Such a posterior temporoparietal pattern of damage chiefly discriminates this syndrome from other subtypes of PPA (Rohrer et al., 2010d).

A VBM study investigated the overlap between the logopenic PPA variant and early age at onset AD by comparing directly patterns of GM atrophy in the two clinical syndromes (Migliaccio et al., 2009). This study showed that, compared to controls, each patient group experiences a large area of overlapping atrophy in the bilateral parietal, occipital, precuneus, posterior cingulate, posterior temporal, and hippocampal regions, with a greater involvement of the left temporal cortex in the logopenic variant. These results agree with the notion that the logopenic variant represents a clinical manifestation of a non-typical form of AD that presents at an early age (Migliaccio et al., 2009).

In logopenic patients, WM volume loss was detected in regions in the vicinity of atrophied GM, such as the posterior portion of the left middle temporal and bilateral posterior–superior temporal gyri (Gorno-Tempini et al., 2008), as well as fornix and along the major long association tracts of the left hemisphere, including the cingulum, SLF, ILF and IFOF (Rohrer et al., 2010d).

Studies evaluating patients with a form of PPA associated with AD pathology demonstrated the presence of temporoparietal atrophy (Table 1) (Grossman et al., 2007a; Josephs et al., 2008). One of these studies showed that the hippocampus was spared (Josephs et al., 2008), while another found hippocampal atrophy (Grossman et al., 2007a). A recent study investigated the value of clinical phenotyping, neuropsychological analysis, and pattern of MRI atrophy in predicting underlying pathology of logopenic cases (Hu et al., 2010). Twelve of 19 patients with the logopenic variant (63%) had neuropathologic findings or CSF biomarkers consistent with AD (Hu et al., 2010). VBM analysis revealed that these patients had a significant posterior–superior temporal atrophy; in case of non-AD pathology, patients experienced

a peri-sylvian atrophy (Fig. 5A) (Hu et al., 2010). Receiver-operator characteristic curve analysis showed that combining neuropsychological testing with the pattern of MRI atrophy allows a 90% specificity to be reached in patients with pathology data or CSF biomarkers consistent with AD (Fig. 5B) (Hu et al., 2010).

Summary

- On structural MRI scans, each PPA variant is associated with a specific pattern of focal atrophy: left frontoinsular and peri-sylvian atrophy in the non-fluent variant, asymmetric atrophy of the anterior temporal and ventromedial frontal lobe in the semantic variant, and left temporoparietal atrophy in logopenic patients.
- Patterns of WM atrophy in PPA patients resemble those seen in GM structures.
- In the logopenic variant, which is the most controversial PPA group, neuropsychological testing and the detection of a pattern of brain atrophy involving the left temporoparietal regions contributes significantly to the diagnostic work up of these patients.

2.2.2. *Atrophy progression (Table 2)*

2.2.2.1. The non-fluent variant. Although atrophy in non-fluent PPA is most prominent in the left inferior frontal regions, the left lateral temporal cortex, anterior parietal lobe and middle and superior parts of the frontal lobe are increasingly affected as the severity of anomia worsens (Rohrer et al., 2009).

To date, only two studies (Gordon et al., 2010; Knopman et al., 2009) quantified the evolution of WB atrophy in non-fluent patients and showed an annual percentage change of 1.7 and 2.6% and a ventricular expansion of 7.4 and 7.1 ml/year, respectively. Unpublished observations suggest that atrophy associated with the non-fluent variant often extends superiorly into the anterior superior temporal lobe, medially into the orbital frontal and anterior cingulate regions, and posteriorly along the Sylvian fissure into the parietal lobe (Grossman, 2010).

Non-fluent PPA can progress to a syndrome encompassing generalised motor problems compatible with a diagnosis of corticobasal syndrome (CBS) or PSP (Josephs et al., 2006). VBM was applied to four annual MRI scans of a 56-year-old woman, whose clinical picture evolved from non-fluent variant to CBS. This study showed a progression of atrophy from the inferior posterior frontal gyrus, to the left insula and finally to the medial frontal lobe (Gorno-Tempini et al., 2004b). The patient died at age 57 and the post-mortem examination revealed a diffuse tau-positive pathology in GM and WM, basal ganglia and substantia nigra, compatible with CBD pathology (Sanchez-Valle et al., 2006). Another study described four patients presenting with non-fluent PPA who subsequently developed features of a PSP syndrome, including a typical oculomotor palsy (Rohrer et al., 2010c). These PSP-non-fluent cases had a less prominent midbrain atrophy but a more marked prefrontal atrophy than the control group consisting of five patients with pathologically confirmed PSP without aphasia. They had, however, a more prominent midbrain atrophy and a less marked peri-sylvian atrophy than other non-fluent cases (Rohrer et al., 2010c).

2.2.2.2. The semantic variant. A cross-sectional study in semantic patients showed that, as the severity of anomia increases, greater cortical thinning of posterior and superior parts of the left temporal lobe, parts of the left frontal lobe (orbitofrontal and inferior gyri), insula and cingulate gyrus can be detected (Fig. 6) (Rohrer et al., 2009). A similar pattern of tissue loss with increasing disease severity was observed in the right temporal lobe of these patients (Rohrer et al., 2009).

A few longitudinal studies assessed the dynamics of global and regional atrophy in semantic patients (Brambati et al., 2009b; Chan et al., 2001a; Gordon et al., 2010; Knopman et al., 2009; Krueger et al., 2010; Rohrer et al., 2008). Using a semiautomated image registration method to calculate annual rates of brain atrophy and VE, several studies found that semantic patients had a greater WB annual percent volume loss (from 1.66% per year to 2.6% per year), and VE (about 7 ml/year) compared with healthy controls (Chan et al., 2001a; Gordon et al., 2010; Knopman et al., 2009; Rohrer et al., 2008). Such changes were independent of age, gender and disease duration (Gordon et al., 2010). Over 1 year, semantic patients had the greatest volume loss in the temporal lobes (5.9% on the left and 4.8% on the right) (Krueger et al., 2010).

Patients who present with predominantly left-sided temporal lobe atrophy develop clinical and radiological features of right temporal lobe damage as the diseases evolve (Fig. 7) (Brambati et al., 2009b; Chan et al., 2001a; Rohrer et al., 2008). In a group of 21 semantic patients, the mean rate of atrophy was 3.9 ml/year in the right temporal lobe versus 2.8 ml/year in the left (Rohrer et al., 2008). Using tensor-based morphometry, both left and right temporal variants of semantic PPA showed a significant progression of GM atrophy over 1 year not only in the temporal lobe most affected at

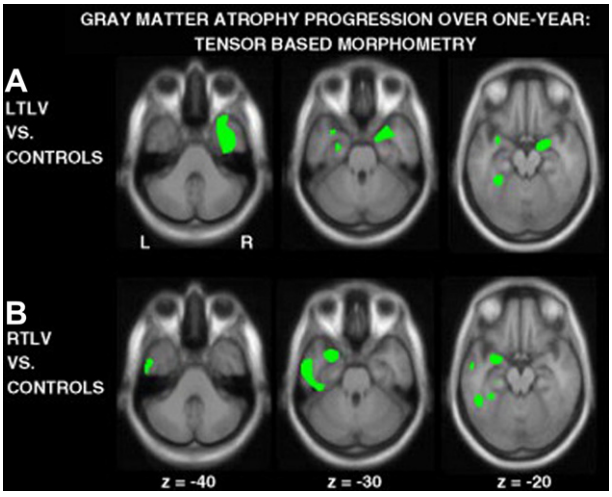

Fig. 7 – A tensor-based morphometry study showing patterns of GM atrophy progression over 1 year in patients with the classic left-lateralised (LTLV) semantic PPA (A), and patients with the right variant of semantic PPA (RTLV) (B) compared with controls. Statistical maps are displayed on sections of the study-specific template used for normalisation. The threshold for display is $p < .05$ corrected for multiple comparisons (family wise error). From Brambati et al. (2009b) with permission.

presentation, but also in the contralateral one (Fig. 7) (Brambati et al., 2009b). In the left variant, progression of volume loss also involved the ventromedial frontal and the left anterior insular regions (Fig. 7A) (Brambati et al., 2009b).

2.2.2.3. The logopenic variant. In logopenic patients, the annualised percent changes were 2.08% for WB volume and 14.78% for VE (Knopman et al., 2009). Regional longitudinal volumetric studies have not been reported yet, but clinical unpublished observations suggest that, as the disease progresses, inferior regions of the temporal lobe are involved, with an extension superiorly into the parietal lobe, and anteriorly, along the Sylvian fissure, into the frontal lobe (Grossman, 2010).

Summary

- Only a few longitudinal studies assessed the dynamics of global and regional atrophy in PPA patients.
- As the diseases evolve, PPA patients show a progression of GM atrophy not only in the regions most affected at presentation, but also in the corresponding contralateral areas.

2.2.3. *Intrinsic tissue abnormalities*

2.2.3.1. The non-fluent variant. In non-fluent patients compared with controls, GM MD was found to be increased in the left posterior inferior and superior frontal lobe, anterior insula, supplementary motor area, and temporal lobe (Whitwell et al., 2011). Only one DT MRI study has investigated the extent of WM damage in the non-fluent variant, and showed a decreased FA in the bilateral SLF and right uncinate compared with controls (Whitwell et al., 2011). However, the ROI-based approach used in this study prevented a definition of the overall pattern of brain WM damage.

2.2.3.2. The semantic variant. The pattern of GM increased MD in semantic patients matches well with the pattern of tissue loss: the most severe alterations are observed in the left hemisphere, particularly in the temporal lobe (Whitwell et al., 2011). GM MD increases are also observed in the insula, and frontal, parietal and occipital lobes, with a left side predominance (Whitwell et al., 2011). In semantic patients, abnormalities of WM tract diffusivity were identified in the major inferior and superior temporal connections of the left hemisphere (Fig. 8), such as the ILF (Agosta et al., 2010; Borroni et al., 2007; Whitwell et al., 2011), uncinate fasciculus (Agosta et al., 2010; Whitwell et al., 2011), IFOF (Borroni et al., 2007), and arcuate (Agosta et al., 2010; Borroni et al., 2007; Whitwell et al., 2011). Left callosal radiations (Borroni et al., 2007), genu of the corpus callosum (Agosta et al., 2010) and posterior cingulate bundle (Whitwell et al., 2011) were also found to be damaged in these patients. On the contrary, the fronto-parietal WM connections are relatively spared (Agosta et al., 2010). Taken together, these findings suggest that a network-level dysfunction of the language system, along with the distribution of GM loss, can be responsible for the combination of impaired and spared functions typical of the semantic variant.

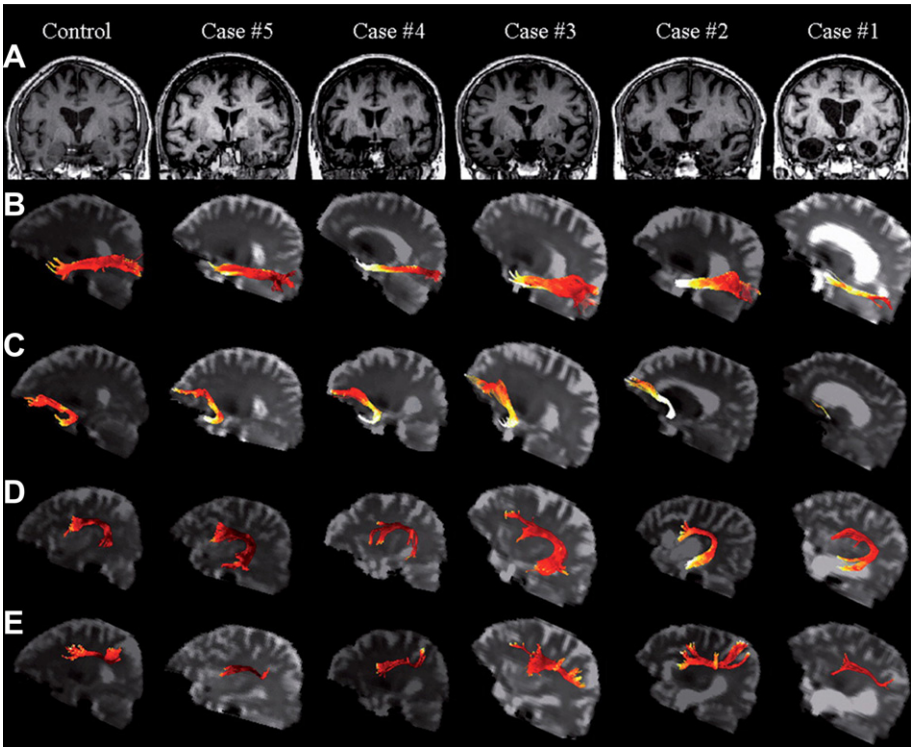

Fig. 8 – (A) Structural MRI of one representative control and each semantic patient studied (coronal view). (B–D) Left language-related white matter tracts are rendered as maps of MD in one representative control and all patients (B: ILF; (C): uncinate fasciculus; (D): arcuate fasciculus; E: fronto-parietal SLF). The colour scale represents the MD values going from lower (dark red) to higher values (yellow to white). Maximum damage is present in the anterior portion of the ILF and uncinate fasciculus underlying the temporal pole. From Agosta et al. (2010) with permission.

2.2.3.3. The logopenic variant

There are currently no DT MRI studies in logopenic patients.

Summary

- The patterns of GM increased MD in non-fluent and semantic patients match well with the patterns of tissue loss.
- The non-fluent variant is associated with an intrinsic damage to the bilateral frontal connections.
- In semantic patients, abnormalities of WM tract diffusivity were detected in all the major inferior and superior temporal connections of the left hemisphere.
- Future studies are warranted to characterize WM changes that may occur in the logopenic variant.

2.2.4. *Clinical correlates*

Using VBM in 51 patients with a neurodegenerative disease presenting with predominant speech and language symptoms, 41 of whom met the criteria for PPA, significant positive correlations were found between scores at four language tasks and regional brain volumes (Amici et al., 2007): deficits in naming were associated with bilateral temporal lobe atrophy; deficits in sentence repetition with atrophy of the left posterior portion of the superior temporal gyrus; deficits in sentence comprehension with left dorsal middle and inferior frontal atrophy; and deficits in fluency with atrophy of the left ventral middle and inferior frontal gyri. A VBM correlation analysis showed a differential pattern of exception and pseudo-word reading abilities in PPA (Brambati et al., 2009a). Exception word reading accuracy, which is typically impaired in semantic patients, correlated with GM volume of the left anterior temporal structures, while pseudo-word reading accuracy, which is typically impaired in logopenic patients, correlated with volume of the left temporoparietal regions (Fig. 9) (Brambati et al., 2009a).

In the non-fluent variant, the classic clinical features are driven by the severity of left frontal and caudate damage. A few VBM studies have thus attempted to identify the specific neural injuries associated with clinical symptoms in non-fluent patients. When compared with non-fluent patients with apraxia of speech (AOS)-only, those with AOS plus dysarthria showed a greater damage to the left face portion of the primary motor cortex and left caudate (Ogar et al., 2007). In non-fluent patients with early mutism, volume loss was more prominent in the pars opercularis and extended into the left basal ganglia (Gorno-Tempini et al., 2006), thus suggesting that damage to the network of brain regions involved in coordination and execution of speech may cause mutism in non-fluent PPA.

In semantic patients, a significant correlation between semantic processing (word/picture matching) and the degree of atrophy of the left anterior temporal lobe has been observed in many studies (Galton et al., 2001; Mummery et al., 2000; Rosen et al., 2002). In a study including both bvFTD and semantic patients, semantic breakdown correlated with extensive GM loss in the left anterior temporal lobe and, less significantly, with atrophy of the right temporal pole and subcallosal gyrus (Williams et al., 2005). Interestingly, a recent study in individuals with a variety of neurodegenerative diseases, including the semantic PPA variant, provided evidence for a differential role of the left and right temporal regions in the extraction of semantic information from verbal and pictorial representations, since material-specific correlations were found between left temporal region volume and verbal stimuli, and right fusiform gyrus volume and non-verbal stimuli (Butler et al., 2009).

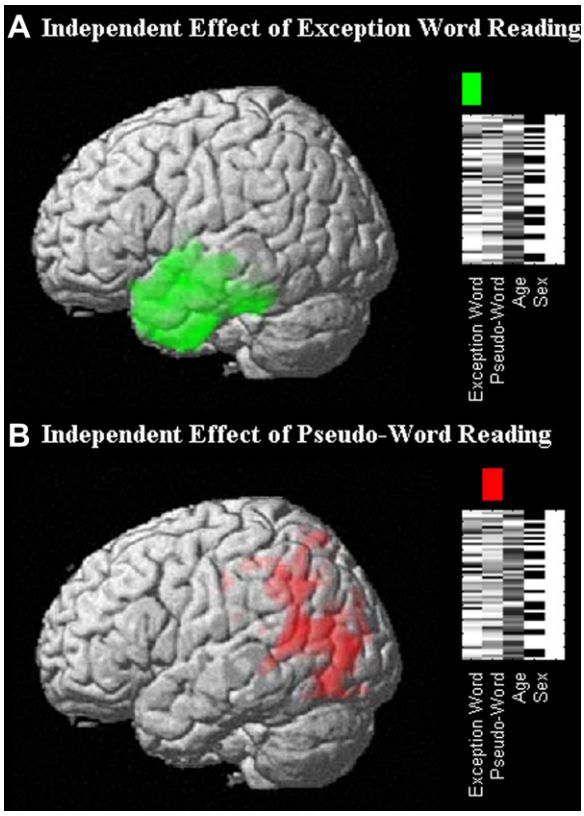

Fig. 9 – VBM study showing brain areas with an independent effect on exception word reading (A), and an independent effect on pseudo-word reading (B) in patients with PPA. Maps of significant correlation are superimposed on the 3D rendering of the Montreal Neurological Institute standard brain. The threshold for display is $p < .05$ corrected for multiple comparisons (family wise error). From Brambati et al. (2009a) with permission.

Abnormal behaviour may develop in PPA patients as the disease evolves, but the anatomical basis of behavioural changes in PPA is not fully understood yet. A VBM study revealed a more severe atrophy of the right orbitofrontal cortex in PPA patients with anxiety, apathy, irritability/lability and abnormal appetite/eating disorders, and a more severe atrophy of the left orbitofrontal cortex in those with disinhibition (Rohrer and Warren, 2010). In semantic patients with predominantly right-sided atrophy, episodic memory, getting lost, and prosopagnosia are associated with a variety of behavioural symptoms including social disinhibition, depression and aggressive behaviour (Chan et al., 2009). Nearly all behavioural symptoms are more prevalent in patients with right temporal lobe atrophy than in those with the classic left-sided semantic dementia (Chan et al., 2009). This suggests that the right temporal variant should be considered as a separate syndromic variant of FTLD.

Longitudinal changes in WB volume and VE in PPA patients were correlated with decline on clinical and cognitive measures, assessed using CDR-SB and MMSE scores respectively (Gordon et al., 2010; Knopman et al., 2009).

Summary

- Specific language deficits in PPA correlate with atrophy of distinct portions of the language network.
- The involvement of the orbitofrontal cortex may be associated with more severe behavioural changes in PPA patients.
- Behavioural symptoms are more prevalent in patients with right temporal lobe atrophy than in those with the classic left-sided semantic PPA.

3. Functional brain alterations in FTLD syndromes

3.1. *bvFTD*

3.1.1. *Brain perfusion and glucose metabolism*

In bvFTD, patterns of hypoperfusion and hypometabolism in frontal, insular, and anterior temporal cortices have been reported (Fig. 10) (Charpentier et al., 2000; Diehl et al., 2004; Franceschi et al., 2005; Ishii et al., 1998; Jeong et al., 2005; Le Ber et al., 2006; Salmon et al., 2003; Sjogren et al., 2000; Varma et al., 2002). The regions mostly impaired are the medial frontal cortex, followed by the frontolateral and anterior temporal cortices. Milder metabolic abnormalities often involve a larger portion of the brain of these patients. The regional analysis of FDG PET images of patients with bvFTD revealed a hypometabolism in the bilateral prefrontal (Diehl et al., 2004; Franceschi et al., 2005; Ishii et al., 1998; Jeong et al., 2005), frontopolar and orbitofrontal cortices (Ishii et al., 1998; Salmon et al., 2003), bilateral insula (Jeong et al., 2005), anterior cingulate cortex (Franceschi et al., 2005; Ishii et al., 1998; Jeong et al., 2005), and left inferior, middle and superior frontal gyri (Ishii et al., 1998). Hypometabolism on FDG PET was also detected in the anterior (Jeong et al., 2005) and medial temporal cortices (Franceschi et al., 2005; Ishii et al., 1998), left inferior parietal gyrus (Jeong et al., 2005), basal ganglia (Diehl et al., 2004; Ishii et al., 1998; Jeong et al., 2005), and thalamus, bilaterally (Franceschi et al., 2005; Ishii et al., 1998; Jeong et al., 2005). Using a voxel-wise principal component analysis on FDG PET images from a large bvFTD population (Salmon et al., 2006), 50% of the metabolic variance was observed in three separate clusters of brain regions: a first metabolic cluster included most of the lateral and medial prefrontal cortex, bilaterally; the two other clusters comprised the subcallosal medial frontal region, temporal pole, medial temporal structures and striatum, in both hemispheres (Salmon et al., 2006).

The regional pattern of predominantly frontal functional impairment in bvFTD usually allows a clear distinction between these patients and those with AD (Charpentier et al., 2000; Ibach et al., 2004; Ishii et al., 1998; Kanda et al., 2008; Sjogren et al., 2000; Varma et al., 2002). However, an overlap of abnormalities between the two conditions can be seen, as AD can involve frontal regions and bvFTD may not spare temporoparietal cortex. Using an anterior-to-posterior cerebral blood flow (CBF) SPECT ratio (medial superior frontal gyrus/medial temporal lobes), bvFTD patients were successfully distinguished from AD patients, with a sensitivity of 87.5%, and a specificity of 96.3% versus early onset AD patients and 80% versus late onset AD patients (Sjogren et al., 2000). A few studies have looked at the accuracy of SPECT or FDG PET findings in relation to the pathological diagnoses (Foster et al., 2007; McNeill et al., 2007). ^{99m}Tc-HMPAO SPECT was obtained from 25 pathologically confirmed cases of bvFTD and 31 patients with pathologically confirmed AD (McNeill et al., 2007). A reduction in frontal CBF was more common in bvFTD than in AD cases and was of diagnostic value

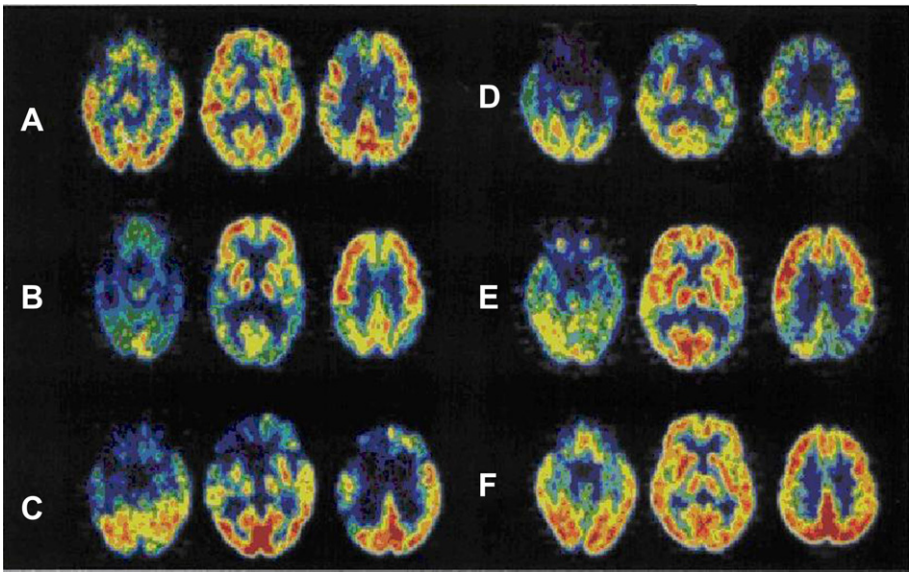

Fig. 10 – (A–D) The typical pattern of cerebral frontotemporal hypometabolism on FDG PET scans in patients with FTLD patients. (E) Bilateral temporoparietal hypometabolism in a patient with AD. (F) Normal glucose metabolism in a cognitively normal subject. From Ishii et al. (1998) [Reprinted by permission of the Society of Nuclear Medicine].

(sensitivity 80%, specificity 65%) (McNeill et al., 2007). When the pattern of bilateral frontal CBF reduction was not associated with a bilateral parietal CBF abnormality, the diagnosis was more accurate (sensitivity 80%, specificity 81%) (McNeill et al., 2007). A recent study of autopsy-proven bvFTD and AD patients showed that the visual interpretation of FDG PET scans after a brief training is more reliable and accurate in distinguishing the two groups than clinical features alone (with more than 85% sensitivity and specificity), even when experienced dementia specialists are involved (Foster et al., 2007). However, unanimity of diagnosis among the raters is more frequent in patients with pathologically confirmed AD than in patients with pathologically confirmed FTLD, and that disagreements in interpretation of scans in patients with FTLD largely occurred when there was temporoparietal hypometabolism (Womack et al., 2010).

In bvFTD, functional changes are likely to progress from anterior-to-posterior brain regions. Le Ber et al. (2006) compared hypoperfusion patterns among bvFTD patients with different disease duration (i.e., <3 years, 3–5 years, and >5 years) and found that early bvFTD is associated with hypoperfusion in the orbitoventral, temporopolar, mesiotemporal, cingular and insular cortices, thalamus and striatum, followed by the involvement of mesial and dorsolateral frontal cortices. Functional abnormalities in posterior parietal and occipital brain regions appeared only at later disease stages (Le Ber et al., 2006). Such a posterior spreading of functional changes in bvFTD patients was also reported by a few longitudinal studies (Diehl-Schmid et al., 2007; Grimmer et al., 2004; Michotte et al., 2001). In an autopsy-proven bvFTD case, baseline FDG PET showed a pattern of prefrontal hypometabolism (Michotte et al., 2001). Eighteen months later, a more extensive involvement of the frontal lobes was detected, as well as hypometabolism of the left parietotemporal cortices (Michotte et al., 2001). These findings were confirmed by a study of 22 bvFTD patients that underwent FDG PET at baseline and after a mean interval of 19.5 months (Diehl-Schmid et al., 2007). At baseline, bvFTD patients showed a symmetrical hypometabolism of the frontal lobes, insula cortex, caudate nuclei, and thalami relative to healthy controls (Diehl-Schmid et al., 2007). After 19.5 months, a worsening of the hypometabolism of the frontal regions that already harboured metabolic abnormalities at baseline, as well as an additional glucose metabolism reduction in the parietal and temporal cortices, were observed (Diehl-Schmid et al., 2007).

In bvFTD, MMSE scores were found to correlate positively with the CBF of the bilateral posterior cingulate cortex, right parahippocampal gyrus, and right insula (Nakano et al., 2006). The same SPECT study (Nakano et al., 2006) also showed that antisocial behavioural symptoms were associated with CBF reduction in the orbitofrontal cortex, bilateral inferior frontal gyri, left anterior cingulate cortex, right caudate nucleus, and left insula. Furthermore, specific patterns of hypoperfusion and hypometabolism were associated with an initial behavioural presentation (Franceschi et al., 2005; Le Ber et al., 2006; Peters et al., 2006). Inertia was associated with predominant medial frontal and cingulate hypoperfusion, whereas patients with disinhibition had a predominant ventromedial prefrontal and temporal hypoperfusion (Le Ber et al., 2006). Franceschi et al. (2005) found that, compared to disinhibited patients, bvFTD apathetic patients had a greater hypometabolism of the dorsolateral frontal cortex, insula and frontal medial cortex. On the contrary, compared to apathetic patients, disinhibited bvFTD patients showed a greater hypometabolism of posterior orbitofrontal cortex, hippocampus, amygdala, inferior temporal cortex, nucleus accumbens, and inferior temporal gyrus (Franceschi et al., 2005). A more recent study suggested that decreased orbitofrontal metabolism is related to both disinhibited and apathetic syndromes in bvFTD (Peters et al., 2006). Disinhibition scores at the NPI scale correlated with hypometabolism of the posterior orbitofrontal cortex (Peters et al., 2006). When apathetic and non-apathetic patients were contrasted, a specific involvement of the posterior orbitofrontal cortex in apathetic subjects was found (Peters et al., 2006). Further investigations of specific network and neurotransmitter abnormalities are needed to understand how the decrease in metabolism of the same brain regions might induce various social maladjustments.

Brainstem hypoperfusion has been associated with a rapid progression of the disease in bvFTD patients (Le Ber et al., 2006). It was suggested that the serotoninergic raphe nuclei that project to the forebrain are directly or indirectly involved in bvFTD and might lead to death, caused by aspiration pneumonia or dysphagia (Le Ber et al., 2006). Additional research is needed to confirm this finding.

Summary

- In bvFTD patients, hypoperfusion and hypometabolism involve the medial and lateral frontal and anterior temporal cortices, and are likely to progress from anterior-to-posterior brain regions.
- Although an overlap of functional abnormalities between bvFTD and AD has been shown to occur, a reduction in frontal perfusion/metabolism is more common in bvFTD than in AD cases.
- The combined assessment of clinical features and FDG PET scans is more reliable and accurate in distinguishing bvFTD from AD cases than the assessment of clinical features in isolation.
- In bvFTD, the same patterns of hypoperfusion and hypometabolism of frontal, insular, temporal and subcortical regions are reported to be associated with various antisocial behavioural symptoms.

3.1.2. *Amyloid imaging using PET*

PIB PET showed promising results in discriminating bvFTD and AD patients. Generally, low cortical ^{11}C-PIB retention was observed in patients with bvFTD (Engler et al., 2008; Rabinovici et al., 2007a; Rowe et al., 2007). Rabinovici et al. (2007a) studied five bvFTD patients, and seven AD patients. While all AD patients experienced an increased PIB retention, three patients with bvFTD and all healthy controls had PIB-negative scans. The retrospective revision of clinical and functional neuroimaging data showed that the two PIB-positive bvFTD patients had a clinical and cognitive picture consistent with either AD or bvFTD, and biparietal hypometabolism on FDG PET. More recently, PIB PET was used to compare 10 clinically diagnosed bvFTD patients with 17 PIB-

positive AD patients and eight PIB-negative healthy controls (Engler et al., 2008). Two bvFTD patients showed a positive PIB retention similar to that of AD cases (Engler et al., 2008). The accurate revision of clinical and neuroimaging data showed that, although one of the PIB-positive patients had a clinical history and an FDG PET scan suggestive of FTLD, the other had a neuropsychological profile which was atypical for bvFTD and developed a global, AD-like cognitive impairment during follow up, thus suggesting a diagnosis of AD with frontal involvement (Engler et al., 2008). Pathologic correlative studies are now warranted to determine whether patients with PIB-positive FTLD represent false positive diagnoses, comorbid FTLD/AD pathology, or AD pathology mimicking an FTLD clinical syndrome.

The short half-life of ^{11}C-PIB requires the PET centre to have a cyclotron, which may ultimately limit the utility of PIB in clinical practice and prompts the use of other agents. ^{18}F-BAY94-9172 is another Aβ ligand, which provides images of similar appearance to those following PIB administration without the inherent limitation of the 20 min half-life that makes the use of PIB potentially problematic in a clinical setting (Rowe et al., 2008). A recent study showed that four of five FTLD patients (two with bvFTD and two with semantic PPA) had no ^{18}F-BAY94-9172 retention, allowing them to be easily distinguished from AD patients who exhibited a significant ligand retention (Rowe et al., 2008). One patient had a mild frontal binding, but the corresponding scan was read as normal by the blinded reviewer and had a neocortical uptake ratio within the normal range (Rowe et al., 2008). Further validation of ^{18}F-BAY94-9172 is now required, including a full characterisation of the metabolism and kinetics of the compound, to determine the most valuable quantification method to be used clinically.

Summary

- Low cortical ^{11}C-PIB retention is observed in patients with bvFTD.
- PIB PET may be useful in the differential diagnosis between bvFTD and AD cases with frontal involvement.

3.1.3. *Functional activations and RS functional activity using MRI*

A fMRI activation study investigated verbal working memory in early bvFTD and found a decreased recruitment of frontal and parietal regions in patients relative to controls (Rombouts et al., 2003). On the contrary, the bvFTD group displayed a stronger cerebellum recruitment, which was interpreted as a sign of possible compensatory mechanisms (Rombouts et al., 2003).

To our knowledge, only one study has explored the RS functional connectivity in patients with bvFTD (Zhou et al., 2010). Using an independent component analysis approach,

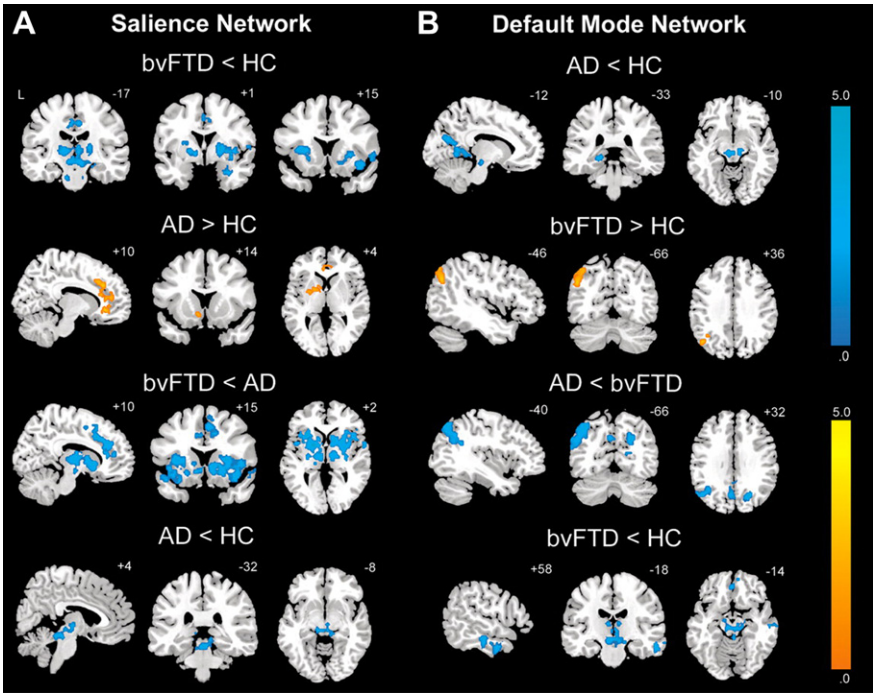

Fig. 11 – Group difference maps showing clusters of significantly reduced or increased RS functional MRI connectivity within the salience network (A) and the DMN, (B) in patients with bvFTD and AD. In the salience network (A), patients with bvFTD showed distributed connectivity reductions compared to healthy controls (HC) and patients with AD, whereas patients with AD showed an increased connectivity in the anterior cingulate cortex and ventral striatum compared to HC. In the DMN (B), patients with AD showed several connectivity impairments compared to HC and patients with bvFTD, whereas patients with bvFTD showed an increased left angular gyrus connectivity. Patients with bvFTD and AD further showed focal brainstem connectivity disruptions within their 'released' network (DMN for bvFTD, salience network for AD). Results are displayed at a joint height and extent probability threshold of $p < .05$, corrected at the WB level. Colour bars represent *t* values, and statistical maps are superimposed on the Montreal Neurological Institute template brain. Adapted from Zhou et al. (2010) with permission.

Zhou et al. (2010) found that, while AD patients have a disrupted connectivity of the default-mode network (DMN), bvFTD is associated with the interruption of the connectivity of the salience network, which is linked to emotional salience processing capacities (Seeley et al., 2007), most notably in the frontal and anterior insula, mid-cingulate and numerous subcortical, limbic and brainstem nodes (Fig. 11). bvFTD patients also experienced an increased left parietal connectivity of the DMN (Zhou et al., 2010). Salience network disruption and DMN enhancement correlate with clinical severity in bvFTD patients (Zhou et al., 2010). A combination of salience network and DMN connectivity scores was found to be able to classify healthy subjects, AD patients, and bvFTD patients with a 92% accuracy, and to separate AD and bvFTD patients with a 100% accuracy (Zhou et al., 2010). This study pioneered the notion that bvFTD may be caused by a degeneration of specific intrinsic functional connectivity networks that are selectively vulnerable to FTLD pathologies. Future work is needed to prove or disprove this intriguing hypothesis.

Summary

- The salience network seems to be selectively vulnerable to FTLD pathology.
- A combination of salience network and DMN connectivity scores could play a role in the diagnostic work up of bvFTD patients.

3.2. PPA

3.2.1. *Brain perfusion and glucose metabolism*

3.2.1.1. The non-fluent variant. A functional deficit of the left frontal or frontotemporal regions of the brain has been reported in non-fluent PPA patients (Fig. 12) (Nestor et al., 2003b; Panegyres et al., 2008; Perneczky et al., 2007; Rabinovici et al., 2008; Zahn et al., 2005). Hypometabolism was found in the left anterior insula/frontal opercular region, and left parahippocampal and fusiform gyri in a group of non-fluent patients with only a small cluster of atrophy in the left perisylvian region on structural MRI scans (Nestor et al., 2003b). A functional involvement of bilateral caudate nuclei and thalami was also described (Perneczky et al., 2007). Reduced parietal cortex function was seen on PET or SPECT scans of non-fluent patients with pathologically confirmed AD compared to non-fluent patients with non-AD pathology (Nestor et al., 2007).

In non-fluent patients, a significant positive correlation was found between the total score of the "Consortium to Establish a Registry for Alzheimer's Disease" Neuropsychological Assessment Battery (CERAD-NAB) and the glucose metabolism of the left striatum and bilateral middle temporal regions (Perneczky et al., 2007); verbal fluency and naming performances were positively associated with the rate of glucose metabolism of the left middle temporal gyrus and left fusiform gyrus (Perneczky et al., 2007). Non-fluent patients with a dominant AOS were characterised by a more superior frontal and supplementary motor cortex hypometabolism (Josephs et al., 2010a). Decreased metabolism in the midbrain, similar to that observed in PSP patients, was found in non-fluent patients with parkinsonism compared with those without (Roh et al., 2010).

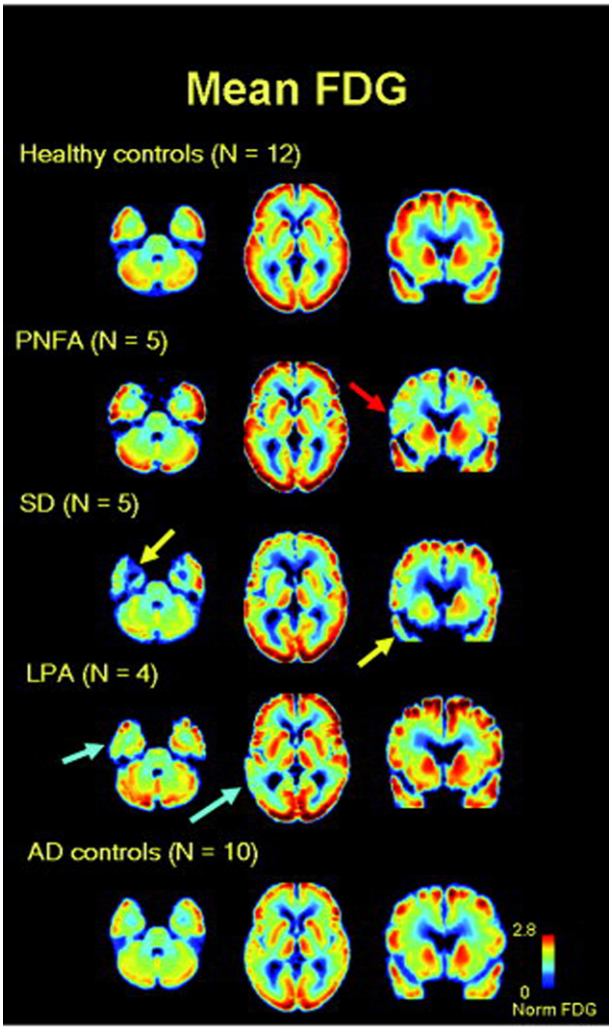

Fig. 12 – FDG PET patterns of abnormalities in PPA variants. Axial and coronal images of mean atrophy-corrected FDG PET from (top to bottom) normal control subjects and non-fluent, semantic, logopenic, and AD patients. Images are in neurological convention. The non-fluent variant is characterised by a left frontal hypometabolism (red arrow), the semantic variant by a left greater than right anterior temporal hypometabolism (yellow arrows), and the logopenic variant by an asymmetric left temporoparietal hypometabolism (light blue arrows). LPA = logopenic progressive aphasia (i.e., logopenic PPA); PNFA = progressive non-fluent aphasia (i.e., non-fluent PPA); SD = semantic dementia (i.e., semantic PPA). From Rabinovici et al. (2008) with permission.

3.2.1.2. The semantic variant. In semantic PPA patients, FDG PET studies showed asymmetrical hypometabolism of the temporal lobes, more marked on the left side (Fig. 12) (Diehl et al., 2004; Drzezga et al., 2008; Nestor et al., 2003a; Rabinovici et al., 2008). A study of patients with semantic PPA and very early AD that combined structural MRI and FDG PET findings revealed hippocampal atrophy and hypometabolism

in both groups (Nestor et al., 2003a). The main difference was a strikingly reduced metabolism in the posterior cingulate cortex in patients with AD that was not present in those with semantic PPA (Nestor et al., 2003a). Another recent observation is that regional atrophy and hypometabolism are closely coupled in semantic PPA but not in AD. That is to say, in semantic patients the anterior temporal regions and connected orbital frontal cortex are both atrophic on MRI and hypometabolic on FDG PET (Diehl et al., 2004). By contrast, AD is characterised by a much more extensive hypometabolism in regions that are not obviously atrophic (Diehl et al., 2004).

Hypometabolism of the anterior fusiform region was found to be strongly associated with semantic scores in a group of 21 FTLD patients with semantic impairment, including 17 patients with semantic PPA and four patients with a mixed syndrome of semantic impairment and behavioural changes (Mion et al., 2010). The left anterior fusiform function predicted performance at two expressive verbal tasks, whereas right anterior fusiform metabolism predicted performance at a non-verbal test of associative semantic knowledge (Mion et al., 2010).

3.2.1.3. The logopenic variant. ^{99m}TC-ethyl cysteinate dimmer SPECT was used in two logopenic patients and showed an hypoperfusion of the left posterior middle and superior temporal and inferior parietal regions relative to healthy controls (Gorno-Tempini et al., 2008). Logopenic patients also experienced a pattern of left posterior temporoparietal hypometabolism on FDG PET scans (Fig. 12) (Rabinovici et al., 2008). A retrospective PET study of PPA patients with AD pathology demonstrated a pattern of temporoparietal involvement similar to that of logopenic patients (Nestor et al., 2007).

Summary
- PPA patients show an asymmetrical pattern of cortical and subcortical hypoperfusion and hypometabolism, more marked on the left side, which may precede the appearance of structural changes.
- Patients with the logopenic variant show a pattern of temporoparietal involvement similar to that seen in AD patients.

3.2.2. *Amyloid imaging using PET*

The first PIB PET report by Rabinovici et al. (2007a) found two PIB-positive out of four semantic patients enrolled in the study. Both patients had FDG PET scans consistent with FTLD. However, one patient had a classic neuropsychological profile for semantic PPA, while the other had a cognitive profile that could be consistent with either AD or FTLD. A more recent study investigating PIB cortical deposition in six non-fluent, five semantic, and four logopenic patients reported that all logopenic cases were PIB-positive, with a pattern of PIB burden similar to that typically observed in AD (Fig. 13) (Rabinovici et al., 2008). On the contrary, PIB uptake was less common in the other PPA variants: a left frontal PIB uptake was seen in only one non-fluent patient, and left temporal uptake in one semantic patient (Fig. 13) (Rabinovici et al., 2008). All eight patients with a clinical diagnosis of the semantic variant studied by Drzezga et al. (2008) were PIB-negative. These findings suggest that amyloid PET imaging may allow characterisation of underlying pathology in PPA patients, but additional studies of larger patients samples are needed to confirm this notion.

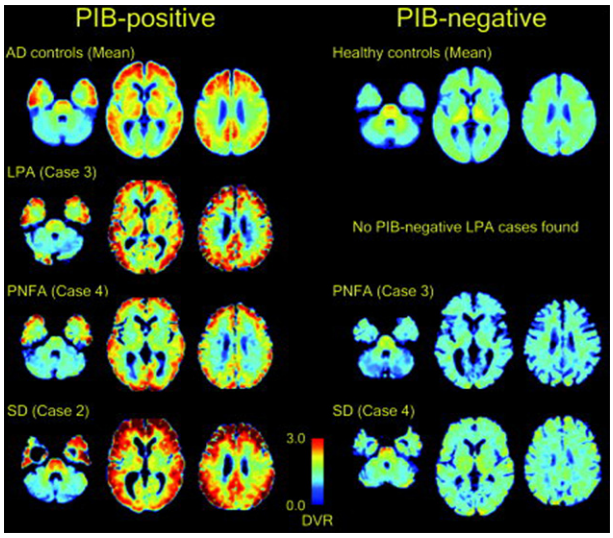

Fig. 13 – Distribution of PIB in PPA variants. Axial slices of normalised, atrophy-corrected PIB distribution volume ratio (DVR) images from individual PIB-positive (left column) and PIB-negative (right column) PPA patients are presented. Identical slices from mean atrophy-corrected PIB DVR images from patients with AD (top left) and healthy control subjects (top right) are shown for comparison. Images are in neurological convention. LPA = logopenic progressive aphasia (i.e., logopenic PPA); PNFA = progressive non-fluent aphasia (i.e., non-fluent PPA); SD = semantic dementia (i.e., semantic PPA). From Rabinovici et al. (2008) with permission.

Summary
- PIB PET may improve the characterisation of the underlying pathology in PPA patients, but additional studies with larger patients samples are needed to confirm this hypothesis.

3.2.3. *Functional activations using MRI*

3.2.3.1. The non-fluent variant. One fMRI study of three non-fluent patients scanned during a sentence comprehension task showed a reduced left inferior frontal activity, but the small sample size did not permit a direct comparison between patients and controls (Cooke et al., 2003). More recently, functional responses to a syntactic comprehension task in eight patients with non-fluent PPA relative to healthy controls were investigated (Wilson et al., 2010). As expected, in controls, the posterior inferior frontal cortex was more recruited with syntactically complex sentences than simpler ones. In non-fluent patients, the posterior inferior frontal cortex was atrophic and, unlike controls, showed an equivalent level of functional activity for syntactically complex and simpler sentences. This study suggests that in non-fluent PPA, the posterior inferior frontal cortex is not only structurally damaged, but also dysfunctional, indicating a critical role of

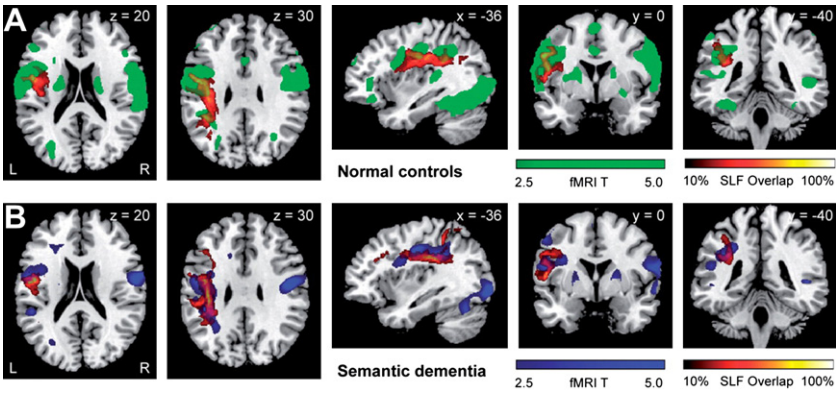

Fig. 14 – Anatomical correspondence between fronto-parietal SLF and functional MRI (fMRI) activation for a contrast which highlights sublexical processing in control subjects (A) and semantic patients (B). fMRI activations for the contrast of low-frequency regular words and pseudowords versus rest are shown in green (A) for healthy controls and in blue (B) for semantic patients. The healthy controls and the semantic patients both showed activation of the posterior inferior frontal gyrus and inferior parietal cortex. Probabilistic maps of the left fronto-parietal SLF obtained in healthy controls (A) and semantic patients (B) are shown in a colour scale which indicates the degree of overlap among subjects. Results are superimposed on the Montreal Neurological Institute standard brain in neurological convention. From Agosta et al. (2010) with permission.

this region in the breakdown of syntactic processing in this syndrome (Wilson et al., 2010).

3.2.3.2. The semantic variant. fMRI was used to investigate the functional anatomy of surface dyslexia in five patients with semantic dementia that were scanned while reading regular words, exception words and pseudowords (Wilson et al., 2009a). In patients, but not in controls, the inferior parietal region was recruited when reading low-frequency exception words. Conversely, the left mid-fusiform and superior temporal regions that showed reading-related activations in controls were not recruited in semantic patients. Intriguingly, a DT MRI tractography study of the same group of patients (Agosta et al., 2010) showed that the ILF and arcuate, which connect the less activated temporal regions, were damaged, while the fronto-parietal SLF, which connects the normally activated posterior inferior frontal and inferior parietal cortices, was spared (Fig. 14). These results (Agosta et al., 2010; Wilson et al., 2009a) suggest that the structural and functional damage to the temporal GM regions and WM connections in semantic patients cause deficits in retrieval of exceptional, item-specific word forms, while the functional and structural sparing of the fronto-parietal network subserves preserved sublexical, phonological processes.

3.2.3.3. The logopenic variant. Using fMRI, PPA patients, likely of the logopenic variant, were examined during both phonological and semantic tasks and showed a general pattern of activation within the classical language network (Sonty et al., 2003). However, PPA patients showed activations, not seen in normals, in the right fusiform gyrus, as well as bilateral precentral gyrus and intra-parietal sulcus. These abnormalities were interpreted as a reflection of compensatory phenomena or as a failure to suppress activity in areas normally inhibited during language tasks (Sonty et al., 2003). A subsequent report by the same group of investigators used dynamic causal modelling analysis and showed a reduced language-specific effective connectivity between Wernicke's and Broca's areas in PPA patients compared with controls (Sonty et al., 2007).

Summary

- The dysfunction of the posterior inferior frontal cortex has a role in the syntactic processing deficits in non-fluent patients; functional alterations of the temporal cortex are associated with surface dyslexia in the semantic variant.
- fMRI studies are likely to contribute to the definition of the neural correlates of the linguistic symptoms of PPA patients.

4. Conclusions and future perspectives

Despite each FTLD variant is associated with characteristic behavioural and/or linguistic features, the fact that they harbour different underlying pathological processes renders the diagnostic work up of these patients a highly challenging task. However, the detection of distinct patterns of atrophy on structural MRI and functional abnormalities on SPECT and PET scans has been shown to contribute at establishing a correct diagnosis of FTLD (Gorno-Tempini et al., 2011; Neary et al., 1998; Rascovsky et al., 2007). These techniques also appear to be useful at distinguishing FTLD from patients with AD (Foster et al., 2007; Rabinovici et al., 2007b). The diagnostic ability of structural and functional imaging techniques is further improved if an image analysis method that provides single-subject classification is employed (Davatzikos et al., 2008; Higdon et al., 2004; Kloppel et al., 2008; Vemuri et al., 2010; Wilson et al., 2009b). Furthermore, a multimodal approach, such one that combines neuropsychological testing and MRI, can improve non-invasive, *in vivo* distinction between FTLD and AD cases (Hu et al., 2010). Nevertheless, it has to be stated that clinical criteria, neuropsychological profiles, and structural and functional imaging may all fail to correctly predict the underlying pathology when this does not adhere to common anatomic patterns. In these cases,

molecular imaging, such as PET with Aβ ligands, may prove to be diriment (Drzezga et al., 2008; Engler et al., 2008; Rabinovici et al., 2007a, 2008; Rowe et al., 2008, 2007).

A major clinical challenge, to date, is the need to improve the prediction of the specific histopathology causing each of the FTLD variants during life. Preliminary studies in pathologically proven cases suggested that distinct patterns of tissue loss could assist in this process (Grossman et al., 2007a; Hu et al., 2010; Josephs et al., 2008, 2010b; Kim et al., 2007; Pereira et al., 2009; Rohrer et al., 2010a, 2010b, 2009; Seelaar et al., 2010; Whitwell et al., 2010, 2005, 2004b). However, the results of these studies are limited by the small numbers of patients assessed. As a consequence, larger ones are needed to verify whether specific patterns of regional atrophy are a signature of specific FTLD pathologies. The discovery of novel radioactive compounds to detect tau or TDP-43 pathology with PET scanning will be central. An improved reliability in distinguishing FTLD pathological variants using neuroimaging techniques may become important in the near future, as aetiology-specific modifying treatments are likely to be developed and entered in the clinical arena.

Rates of cerebral atrophy measured using serial MRI have increasingly become useful markers of disease progression in neurodegenerative disorders, such as AD, and are being used as outcome measures in clinical trials (Fox et al., 2005; Jack et al., 2003). Increased rates of WB atrophy in FTLD patients compared with healthy controls and AD patients have been shown (Chan et al., 2009; Gordon et al., 2010; Knopman et al., 2009; Rohrer et al., 2008; Whitwell et al., 2008, 2007a), which correlated with changes in clinical and cognitive measures (Gordon et al., 2010; Knopman et al., 2009). In two studies the use of serial MRI scans required smaller sample sizes to achieve a significant effect than clinical rating scales (Gordon et al., 2010; Knopman et al., 2009). Larger longitudinal studies will be essential to validate the use of WB volume measurements for the assessment of disease modifying treatments in FTLD. Furthermore, a large-scale application of advanced MRI techniques assessing the regional distribution of tissue loss in multicentre studies may help to identify regions that would provide the most sensitive outcome measures in clinical trials of patients with FTLD.

Along with the well-documented GM changes, WM damage in FTLD has been investigated systematically by recent studies. DT MRI has been shown to be sensitive to structural WM changes in FTLD (Agosta et al., 2010; Borroni et al., 2007; Matsuo et al., 2008; Whitwell et al., 2011; Zhang et al., 2009) and holds promise for detecting and quantifying the intrinsic abnormalities that accompany macrostructural loss of tissue in FTLD syndromes. Furthermore, DT MRI could elucidate the earliest point at which structural changes occur in FTLD by focussing on patients with normal structural MRI scans. However, whether WM abnormalities are reliable diagnostic biomarkers for FTLD syndromes still needs to be proved (Avants et al., 2010; Zhang et al., 2009).

Little is known regarding task-related functional activity of FTLD patients (Cooke et al., 2003; Rombouts et al., 2003; Sonty et al., 2003, 2007; Wilson et al., 2009a, 2010). In this context, studies of larger patient samples are warranted to clarify the neural correlates of the behavioural and linguistic symptoms of FTLD patients. The main problem in the interpretation of fMRI studies in cognitively diseased people is that the observed changes might be biased by disease-driven differences in task performance between patients and controls. On the contrary, RS fMRI makes no demand on subject other than holding still and, as a consequence, can be acquired in patients that are unable to perform a task-associated fMRI. RS fMRI has provided new insights into the cortical abnormalities of patients with bvFTD (Zhou et al., 2010), and should be used to increasingly investigate the nature of the language network impairment in PPA patients. Furthermore, the application of RS fMRI in healthy subjects carrying a genetic risk for FTLD may clarify whether the disease modulates brain function years before any structural or clinical expression of the underlying neurodegenerative process. Finally, there is currently no study combining RS fMRI and DT MRI data in FTLD patients. Such an analysis would offer the unique opportunity to improve our understanding of the structural basis underlying brain functional changes in this condition.

REFERENCES

Agosta F, Henry RG, Migliaccio R, Neuhaus J, Miller BL, Dronkers NF, et al. Language networks in semantic dementia. *Brain*, 133(Pt 1): 286–299, 2010.

Amici S, Ogar J, Brambati SM, Miller BL, Neuhaus J, Dronkers NL, et al. Performance in specific language tasks correlates with regional volume changes in progressive aphasia. *Cognitive and Behavioral Neurology*, 20(4): 203–211, 2007.

Avants BB, Cook PA, Ungar L, Gee JC, and Grossman M. Dementia induces correlated reductions in white matter integrity and cortical thickness: A multivariate neuroimaging study with sparse canonical correlation analysis. *NeuroImage*, 50(3): 1004–1016, 2010.

Barnes J, Godbolt AK, Frost C, Boyes RG, Jones BF, Scahill RI, et al. Atrophy rates of the cingulate gyrus and hippocampus in AD and FTLD. *Neurobiology of Aging*, 28(1): 20–28, 2007.

Barnes J, Whitwell JL, Frost C, Josephs KA, Rossor M, and Fox NC. Measurements of the amygdala and hippocampus in pathologically confirmed Alzheimer disease and frontotemporal lobar degeneration. *Archives of Neurology*, 63(10): 1434–1439, 2006.

Boccardi M, Laakso MP, Bresciani L, Galluzzi S, Geroldi C, Beltramello A, et al. The MRI pattern of frontal and temporal brain atrophy in fronto-temporal dementia. *Neurobiology of Aging*, 24(1): 95–103, 2003.

Boccardi M, Sabattoli F, Laakso MP, Testa C, Rossi R, Beltramello A, et al. Frontotemporal dementia as a neural system disease. *Neurobiology of Aging*, 26(1): 37–44, 2005.

Borroni B, Brambati SM, Agosti C, Gipponi S, Bellelli G, Gasparotti R, et al. Evidence of white matter changes on diffusion tensor imaging in frontotemporal dementia. *Archives of Neurology*, 64(2): 246–251, 2007.

Boxer AL, Rankin KP, Miller BL, Schuff N, Weiner M, Gorno-Tempini ML, et al. Cinguloparietal atrophy distinguishes Alzheimer disease from semantic dementia. *Archives of Neurology*, 60(7): 949–956, 2003.

Brambati SM, Ogar J, Neuhaus J, Miller BL, and Gorno-Tempini ML. Reading disorders in primary progressive aphasia: A behavioral and neuroimaging study. *Neuropsychologia*, 47(8–9): 1893–1900, 2009a.

Brambati SM, Rankin KP, Narvid J, Seeley WW, Dean D, Rosen HJ, et al. Atrophy progression in semantic dementia with asymmetric temporal involvement: A tensor-based

morphometry study. *Neurobiology of Aging*, 30(1): 103–111, 2009b.
Brambati SM, Renda NC, Rankin KP, Rosen HJ, Seeley WW, Ashburner J, et al. A tensor based morphometry study of longitudinal gray matter contraction in FTD. *NeuroImage*, 35(3): 998–1003, 2007.
Butler CR, Brambati SM, Miller BL, and Gorno-Tempini ML. The neural correlates of verbal and nonverbal semantic processing deficits in neurodegenerative disease. *Cognitive and Behavioral Neurology*, 22(2): 73–80, 2009.
Cardenas VA, Boxer AL, Chao LL, Gorno-Tempini ML, Miller BL, Weiner MW, et al. Deformation-based morphometry reveals brain atrophy in frontotemporal dementia. *Archives of Neurology*, 64(6): 873–877, 2007.
Chan D, Anderson V, Pijnenburg Y, Whitwell J, Barnes J, Scahill R, et al. The clinical profile of right temporal lobe atrophy. *Brain*, 132(Pt 5): 1287–1298, 2009.
Chan D, Fox NC, Jenkins R, Scahill RI, Crum WR, and Rossor MN. Rates of global and regional cerebral atrophy in AD and frontotemporal dementia. *Neurology*, 57(10): 1756–1763, 2001a.
Chan D, Fox NC, Scahill RI, Crum WR, Whitwell JL, Leschziner G, et al. Patterns of temporal lobe atrophy in semantic dementia and Alzheimer's disease. *Annals of Neurology*, 49(4): 433–442, 2001b.
Chao LL, Schuff N, Clevenger EM, Mueller SG, Rosen HJ, Gorno-Tempini ML, et al. Patterns of white matter atrophy in frontotemporal lobar degeneration. *Archives of Neurology*, 64(11): 1619–1624, 2007.
Charpentier P, Lavenu I, Defebvre L, Duhamel A, Lecouffe P, Pasquier F, et al. Alzheimer's disease and frontotemporal dementia are differentiated by discriminant analysis applied to (99m)Tc HmPAO SPECT data. *Journal of Neurology, Neurosurgery & Psychiatry*, 69(5): 661–663, 2000.
Cooke A, DeVita C, Gee J, Alsop D, Detre J, Chen W, et al. Neural basis for sentence comprehension deficits in frontotemporal dementia. *Brain and Language*, 85(2): 211–221, 2003.
Davatzikos C, Resnick SM, Wu X, Parmpi P, and Clark CM. Individual patient diagnosis of AD and FTD via high-dimensional pattern classification of MRI. *NeuroImage*, 41(4): 1220–1227, 2008.
Diehl-Schmid J, Grimmer T, Drzezga A, Bornschein S, Riemenschneider M, Forstl H, et al. Decline of cerebral glucose metabolism in frontotemporal dementia: A longitudinal 18F-FDG-PET-study. *Neurobiology of Aging*, 28(1): 42–50, 2007.
Diehl J, Grimmer T, Drzezga A, Riemenschneider M, Forstl H, and Kurz A. Cerebral metabolic patterns at early stages of frontotemporal dementia and semantic dementia. A PET study. *Neurobiology of Aging*, 25(8): 1051–1056, 2004.
Drzezga A, Grimmer T, Henriksen G, Stangier I, Perneczky R, Diehl-Schmid J, et al. Imaging of amyloid plaques and cerebral glucose metabolism in semantic dementia and Alzheimer's disease. *NeuroImage*, 39(2): 619–633, 2008.
Du AT, Schuff N, Kramer JH, Rosen HJ, Gorno-Tempini ML, Rankin K, et al. Different regional patterns of cortical thinning in Alzheimer's disease and frontotemporal dementia. *Brain*, 130(Pt 4): 1159–1166, 2007.
Engler H, Santillo AF, Wang SX, Lindau M, Savitcheva I, Nordberg A, et al. In vivo amyloid imaging with PET in frontotemporal dementia. *European Journal of Nuclear Medicine and Molecular Imaging*, 35(1): 100–106, 2008.
Foster NL, Heidebrink JL, Clark CM, Jagust WJ, Arnold SE, Barbas NR, et al. FDG-PET improves accuracy in distinguishing frontotemporal dementia and Alzheimer's disease. *Brain*, 130(Pt 10): 2616–2635, 2007.
Fox NC, Black RS, Gilman S, Rossor MN, Griffith SG, Jenkins L, et al. Effects of Abeta immunization (AN1792) on MRI measures of cerebral volume in Alzheimer disease. *Neurology*, 64(9): 1563–1572, 2005.
Franceschi M, Anchisi D, Pelati O, Zuffi M, Matarrese M, Moresco RM, et al. Glucose metabolism and serotonin receptors in the frontotemporal lobe degeneration. *Annals of Neurology*, 57(2): 216–225, 2005.
Galton CJ, Patterson K, Graham K, Lambon-Ralph MA, Williams G, Antoun N, et al. Differing patterns of temporal atrophy in Alzheimer's disease and semantic dementia. *Neurology*, 57(2): 216–225, 2001.
Garibotto V, Borroni B, Agosti C, Premi E, Alberici A, Eickhoff SB, et al. Subcortical and deep cortical atrophy in frontotemporal lobar degeneration. *Neurobiology of Aging*, 32(5): 875–884, 2011.
Gordon E, Rohrer JD, Kim LG, Omar R, Rossor MN, Fox NC, et al. Measuring disease progression in frontotemporal lobar degeneration: A clinical and MRI study. *Neurology*, 74(8): 666–673, 2010.
Gorno-Tempini ML, Brambati SM, Ginex V, Ogar J, Dronkers NF, Marcone A, et al. The logopenic/phonological variant of primary progressive aphasia. *Neurology*, 71(16): 1227–1234, 2008.
Gorno-Tempini ML, Dronkers NF, Rankin KP, Ogar JM, Phengrasamy L, Rosen HJ, et al. Cognition and anatomy in three variants of primary progressive aphasia. *Annals of Neurology*, 55(3): 335–346, 2004a.
Gorno-Tempini ML, Hillis AE, Weintraub S, Kertesz A, Mendez M, Cappa SF, et al. Classification of primary progressive aphasia and its variants. *Neurology*, 76(11): 1006–1014, 2011.
Gorno-Tempini ML, Murray RC, Rankin KP, Weiner MW, and Miller BL. Clinical, cognitive and anatomical evolution from nonfluent progressive aphasia to corticobasal syndrome: A case report. *Neurocase*, 10(6): 426–436, 2004b.
Gorno-Tempini ML, Ogar JM, Brambati SM, Wang P, Jeong JH, Rankin KP, et al. Anatomical correlates of early mutism in progressive nonfluent aphasia. *Neurology*, 67(10): 1849–1851, 2006.
Greicius MD, Srivastava G, Reiss AL, and Menon V. Default-mode network activity distinguishes Alzheimer's disease from healthy aging: Evidence from functional MRI. *Proceedings of the National Academy of Sciences of the United States of America*, 101(13): 4637–4642, 2004.
Grimmer T, Diehl J, Drzezga A, Forstl H, and Kurz A. Region-specific decline of cerebral glucose metabolism in patients with frontotemporal dementia: A prospective 18F-FDG-PET study. *Dementia and Geriatric Cognitive Disorders*, 18(1): 32–36, 2004.
Grossman M. Biomarkers in frontotemporal lobar degeneration. *Current Opinion in Neurology*, 23(6): 643–648, 2010.
Grossman M, Libon DJ, Forman MS, Massimo L, Wood E, Moore P, et al. Distinct antemortem profiles in patients with pathologically defined frontotemporal dementia. *Archives of Neurology*, 64(11): 1601–1609, 2007a.
Grossman M, Wood EM, Moore P, Neumann M, Kwong L, Forman MS, et al. TDP-43 pathologic lesions and clinical phenotype in frontotemporal lobar degeneration with ubiquitin-positive inclusions. *Archives of Neurology*, 64(10): 1449–1454, 2007b.
Higdon R, Foster NL, Koeppe RA, DeCarli CS, Jagust WJ, Clark CM, et al. A comparison of classification methods for differentiating fronto-temporal dementia from Alzheimer's disease using FDG-PET imaging. *Statistics in Medicine*, 23(2): 315–326, 2004.
Hodges JR, Davies RR, Xuereb JH, Casey B, Broe M, Bak TH, et al. Clinicopathological correlates in frontotemporal dementia. *Annals of Neurology*, 56(3): 399–406, 2004.
Hodges JR, Patterson K, Oxbury S, and Funnell E. Semantic dementia. Progressive fluent aphasia with temporal lobe atrophy. *Brain*, 115(Pt 6): 1783–1806, 1992.
Hu WT, McMillan C, Libon D, Leight S, Forman M, Lee VM, et al. Multimodal predictors for Alzheimer disease in nonfluent primary progressive aphasia. *Neurology*, 75(7): 595–602, 2010.
Ibach B, Poljansky S, Marienhagen J, Sommer M, Manner P, and Hajak G. Contrasting metabolic impairment in frontotemporal

degeneration and early onset Alzheimer's disease. *NeuroImage*, 23(2): 739–743, 2004.
Ishii K, Sakamoto S, Sasaki M, Kitagaki H, Yamaji S, Hashimoto M, et al. Cerebral glucose metabolism in patients with frontotemporal dementia. *The Journal of Nuclear Medicine*, 39(11): 1875–1878, 1998.
Jack Jr CR, Slomkowski M, Gracon S, Hoover TM, Felmlee JP, Stewart K, et al. MRI as a biomarker of disease progression in a therapeutic trial of milameline for AD. *Neurology*, 60(2): 253–260, 2003.
Jeong Y, Cho SS, Park JM, Kang SJ, Lee JS, Kang E, et al. 18F-FDG PET findings in frontotemporal dementia: An SPM analysis of 29 patients. *The Journal of Nuclear Medicine*, 46(2): 233–239, 2005.
Josephs KA, Duffy JR, Fossett TR, Strand EA, Claassen DO, Whitwell JL, et al. Fluorodeoxyglucose F18 positron emission tomography in progressive apraxia of speech and primary progressive aphasia variants. *Archives of Neurology*, 67(5): 596–605, 2010a.
Josephs KA, Duffy JR, Strand EA, Whitwell JL, Layton KF, Parisi JE, et al. Clinicopathological and imaging correlates of progressive aphasia and apraxia of speech. *Brain*, 129(Pt 6): 1385–1398, 2006.
Josephs KA, Whitwell JL, Duffy JR, Vanvoorst WA, Strand EA, Hu WT, et al. Progressive aphasia secondary to Alzheimer disease vs FTLD pathology. *Neurology*, 70(1): 25–34, 2008.
Josephs KA, Whitwell JL, Parisi JE, Petersen RC, Boeve BF, Jack Jr CR, et al. Caudate atrophy on MRI is a characteristic feature of FTLD-FUS. *European Journal of Neurology*, 17(7): 969–975, 2010b.
Kanda T, Ishii K, Uemura T, Miyamoto N, Yoshikawa T, Kono AK, et al. Comparison of grey matter and metabolic reductions in frontotemporal dementia using FDG-PET and voxel-based morphometric MR studies. *European Journal of Nuclear Medicine and Molecular Imaging*, 35(12): 2227–2234, 2008.
Kim EJ, Rabinovici GD, Seeley WW, Halabi C, Shu H, Weiner MW, et al. Patterns of MRI atrophy in tau positive and ubiquitin positive frontotemporal lobar degeneration. *Journal of Neurology, Neurosurgery & Psychiatry*, 78(12): 1375–1378, 2007.
Kloppel S, Stonnington CM, Chu C, Draganski B, Scahill RI, Rohrer JD, et al. Automatic classification of MR scans in Alzheimer's disease. *Brain*, 131(Pt 3): 681–689, 2008.
Klunk WE, Engler H, Nordberg A, Wang Y, Blomqvist G, Holt DP, et al. Imaging brain amyloid in Alzheimer's disease with Pittsburgh Compound-B. *Annals of Neurology*, 55(3): 306–319, 2004.
Knibb JA, Xuereb JH, Patterson K, and Hodges JR. Clinical and pathological characterization of progressive aphasia. *Annals of Neurology*, 59(1): 156–165, 2006.
Knopman DS, Jack Jr CR, Kramer JH, Boeve BF, Caselli RJ, Graff-Radford NR, et al. Brain and ventricular volumetric changes in frontotemporal lobar degeneration over 1 year. *Neurology*, 72(21): 1843–1849, 2009.
Krueger CE, Dean DL, Rosen HJ, Halabi C, Weiner M, Miller BL, et al. Longitudinal rates of lobar atrophy in frontotemporal dementia, semantic dementia, and Alzheimer's disease. *Alzheimer Disease and Associated Disorders*, 24(1): 43–48, 2010.
Larsson EM, Englund E, Sjobeck M, Latt J, and Brockstedt S. MRI with diffusion tensor imaging post-mortem at 3.0 T in a patient with frontotemporal dementia. *Dementia and Geriatric Cognitive Disorders*, 17(4): 316–319, 2004.
Le Ber I, Guedj E, Gabelle A, Verpillat P, Volteau M, Thomas-Anterion C, et al. Demographic, neurological and behavioural characteristics and brain perfusion SPECT in frontal variant of frontotemporal dementia. *Brain*, 129(Pt 11): 3051–3065, 2006.
Likeman M, Anderson VM, Stevens JM, Waldman AD, Godbolt AK, Frost C, et al. Visual assessment of atrophy on magnetic resonance imaging in the diagnosis of pathologically confirmed young-onset dementias. *Archives of Neurology*, 62(9): 1410–1415, 2005.
Mackenzie IR, Baborie A, Pickering-Brown S, Du Plessis D, Jaros E, Perry RH, et al. Heterogeneity of ubiquitin pathology in frontotemporal lobar degeneration: Classification and relation to clinical phenotype. *Acta Neuropathologica*, 112(5): 539–549, 2006.
Mackenzie IR, Neumann M, Bigio EH, Cairns NJ, Alafuzoff I, Kril J, et al. Nomenclature and nosology for neuropathologic subtypes of frontotemporal lobar degeneration: An update. *Acta Neuropathologica*, 119(1): 1–4, 2010.
Massimo L, Powers C, Moore P, Vesely L, Avants B, Gee J, et al. Neuroanatomy of apathy and disinhibition in frontotemporal lobar degeneration. *Dementia and Geriatric Cognitive Disorders*, 27(1): 96–104, 2009.
Matsuo K, Mizuno T, Yamada K, Akazawa K, Kasai T, Kondo M, et al. Cerebral white matter damage in frontotemporal dementia assessed by diffusion tensor tractography. *Neuroradiology*, 50(7): 605–611, 2008.
McNeill R, Sare GM, Manoharan M, Testa HJ, Mann DM, Neary D, et al. Accuracy of single-photon emission computed tomography in differentiating frontotemporal dementia from Alzheimer's disease. *Journal of Neurology, Neurosurgery & Psychiatry*, 78(4): 350–355, 2007.
Mesulam M, Wicklund A, Johnson N, Rogalski E, Leger GC, Rademaker A, et al. Alzheimer and frontotemporal pathology in subsets of primary progressive aphasia. *Annals of Neurology*, 63(6): 709–719, 2008.
Mesulam MM. Primary progressive aphasia. *Annals of Neurology*, 49(4): 425–432, 2001.
Michotte A, Goldman S, Tugendhaft P, and Zegers de Beyl D. Frontotemporal dementia: A clinical-pathological study. *Acta Neurologica Belgica*, 101(4): 224–229, 2001.
Migliaccio R, Agosta F, Rascovsky K, Karydas A, Bonasera S, Rabinovici GD, et al. Clinical syndromes associated with posterior atrophy: Early age at onset AD spectrum. *Neurology*, 73(19): 1571–1578, 2009.
Mion M, Patterson K, Acosta-Cabronero J, Pengas G, Izquierdo-Garcia D, Hong YT, et al. What the left and right anterior fusiform gyri tell us about semantic memory. *Brain*, 133(11): 3256–3268, 2010.
Mummery CJ, Patterson K, Price CJ, Ashburner J, Frackowiak RS, and Hodges JR. A voxel-based morphometry study of semantic dementia: Relationship between temporal lobe atrophy and semantic memory. *Annals of Neurology*, 47(1): 36–45, 2000.
Mummery CJ, Patterson K, Wise RJ, Vandenberghe R, Price CJ, and Hodges JR. Disrupted temporal lobe connections in semantic dementia. *Brain*, 122(Pt 1): 61–73, 1999.
Nakano S, Asada T, Yamashita F, Kitamura N, Matsuda H, Hirai S, et al. Relationship between antisocial behavior and regional cerebral blood flow in frontotemporal dementia. *NeuroImage*, 32(1): 301–306, 2006.
Neary D, Snowden JS, Gustafson L, Passant U, Stuss D, Black S, et al. Frontotemporal lobar degeneration: A consensus on clinical diagnostic criteria. *Neurology*, 51(6): 1546–1554, 1998.
Nestor PJ, Balan K, Cheow HK, Fryer TD, Knibb JA, Xuereb JH, et al. Nuclear imaging can predict pathologic diagnosis in progressive nonfluent aphasia. *Neurology*, 68(3): 238–239, 2007.
Nestor PJ, Fryer TD, Ikeda M, and Hodges JR. Retrosplenial cortex (BA 29/30) hypometabolism in mild cognitive impairment (prodromal Alzheimer's disease). *European Journal of Neuroscience*, 18(9): 2663–2667, 2003a.
Nestor PJ, Graham NL, Fryer TD, Williams GB, Patterson K, and Hodges JR. Progressive non-fluent aphasia is associated with hypometabolism centred on the left anterior insula. *Brain*, 126(Pt 11): 2406–2418, 2003b.
Ogar JM, Dronkers NF, Brambati SM, Miller BL, and Gorno-Tempini ML. Progressive nonfluent aphasia and its characteristic motor speech deficits. *Alzheimer Disease and Associated Disorders*, 21(4): S23–S30, 2007.

Panegyres PK, McCarthy M, Campbell A, Lenzo N, Fallon M, and Thompson J. Correlative studies of structural and functional imaging in primary progressive aphasia. *American Journal of Alzheimer's Disease and Other Dementias*, 23(2): 184–191, 2008.

Pereira JM, Williams GB, Acosta-Cabronero J, Pengas G, Spillantini MG, Xuereb JH, et al. Atrophy patterns in histologic vs clinical groupings of frontotemporal lobar degeneration. *Neurology*, 72(19): 1653–1660, 2009.

Perneczky R, Diehl-Schmid J, Pohl C, Drzezga A, and Kurz A. Non-fluent progressive aphasia: Cerebral metabolic patterns and brain reserve. *Brain Research*, 1133(1): 178–185, 2007.

Perry RJ, Graham A, Williams G, Rosen H, Erzinclioglu S, Weiner M, et al. Patterns of frontal lobe atrophy in frontotemporal dementia: A volumetric MRI study. *Dementia and Geriatric Cognitive Disorders*, 22(4): 278–287, 2006.

Peters F, Perani D, Herholz K, Holthoff V, Beuthien-Baumann B, Sorbi S, et al. Orbitofrontal dysfunction related to both apathy and disinhibition in frontotemporal dementia. *Dementia and Geriatric Cognitive Disorders*, 21(5–6): 373–379, 2006.

Pierpaoli C, Jezzard P, Basser PJ, Barnett A, and Di Chiro G. Diffusion tensor MR imaging of the human brain. *Radiology*, 201(3): 637–648, 1996.

Piguet O, Petersen A, Yin Ka Lam B, Gabery S, Murphy K, Hodges JR, et al. Eating and hypothalamus changes in behavioral-variant frontotemporal dementia. *Annals of Neurology*, 69(2): 312–319, 2011.

Rabinovici GD, Furst AJ, O'Neil JP, Racine CA, Mormino EC, Baker SL, et al. 11C-PIB PET imaging in Alzheimer disease and frontotemporal lobar degeneration. *Neurology*, 68(15): 1205–1212, 2007a.

Rabinovici GD, Jagust WJ, Furst AJ, Ogar JM, Racine CA, Mormino EC, et al. Abeta amyloid and glucose metabolism in three variants of primary progressive aphasia. *Annals of Neurology*, 64(4): 388–401, 2008.

Rabinovici GD and Miller BL. Frontotemporal lobar degeneration: Epidemiology, pathophysiology, diagnosis and management. *CNS Drugs*, 24(5): 375–398, 2010.

Rabinovici GD, Seeley WW, Kim EJ, Gorno-Tempini ML, Rascovsky K, Pagliaro TA, et al. Distinct MRI atrophy patterns in autopsy-proven Alzheimer's disease and frontotemporal lobar degeneration. *American Journal of Alzheimer's Disease and Other Dementias*, 22(6): 474–488, 2007b.

Rascovsky K, Hodges JR, Kipps CM, Johnson JK, Seeley WW, Mendez MF, et al. Diagnostic criteria for the behavioral variant of frontotemporal dementia (bvFTD): Current limitations and future directions. *Alzheimer Disease and Associated Disorders*, 21(4): S14–S18, 2007.

Richards BA, Chertkow H, Singh V, Robillard A, Massoud F, Evans AC, et al. Patterns of cortical thinning in Alzheimer's disease and frontotemporal dementia. *Neurobiology of Aging*, 30(10): 1626–1636, 2009.

Roh JH, Suh MK, Kim EJ, Go SM, Na DL, and Seo SW. Glucose metabolism in progressive nonfluent aphasia with and without parkinsonism. *Neurology*, 75(11): 1022–1024, 2010.

Rohrer JD, Geser F, Zhou J, Gennatas ED, Sidhu M, Trojanowski JQ, et al. TDP-43 subtypes are associated with distinct atrophy patterns in frontotemporal dementia. *Neurology*, 75(24): 2204–2211, 2010a.

Rohrer JD, Lashley T, Holton J, Revesz T, Urwin H, Isaacs AM, et al. The clinical and neuroanatomical phenotype of FUS associated frontotemporal lobar degeneration. *Journal of Neurology, Neurosurgery & Psychiatry*. Epub ahead of print 2010b.

Rohrer JD, McNaught E, Foster J, Clegg SL, Barnes J, Omar R, et al. Tracking progression in frontotemporal lobar degeneration: Serial MRI in semantic dementia. *Neurology*, 71(18): 1445–1451, 2008.

Rohrer JD, Paviour D, Bronstein AM, O'Sullivan SS, Lees A, and Warren JD. Progressive supranuclear palsy syndrome presenting as progressive nonfluent aphasia: A neuropsychological and neuroimaging analysis. *Movement Disorders*, 25(2): 179–188, 2010c.

Rohrer JD, Ridgway GR, Crutch SJ, Hailstone J, Goll JC, Clarkson MJ, et al. Progressive logopenic/phonological aphasia: Erosion of the language network. *NeuroImage*, 49(1): 984–993, 2010d.

Rohrer JD and Warren JD. Phenomenology and anatomy of abnormal behaviours in primary progressive aphasia. *Journal of the Neurological Sciences*, 293(1–2): 35–38, 2010.

Rohrer JD, Warren JD, Modat M, Ridgway GR, Douiri A, Rossor MN, et al. Patterns of cortical thinning in the language variants of frontotemporal lobar degeneration. *Neurology*, 72(18): 1562–1569, 2009.

Rombouts SA, van Swieten JC, Pijnenburg YA, Goekoop R, Barkhof F, and Scheltens P. Loss of frontal fMRI activation in early frontotemporal dementia compared to early AD. *Neurology*, 60(12): 1904–1908, 2003.

Rosen HJ, Allison SC, Schauer GF, Gorno-Tempini ML, Weiner MW, and Miller BL. Neuroanatomical correlates of behavioural disorders in dementia. *Brain*, 128(Pt 11): 2612–2625, 2005.

Rosen HJ, Gorno-Tempini ML, Goldman WP, Perry RJ, Schuff N, Weiner M, et al. Patterns of brain atrophy in frontotemporal dementia and semantic dementia. *Neurology*, 58(2): 198–208, 2002.

Rowe CC, Ackerman U, Browne W, Mulligan R, Pike KL, O'Keefe G, et al. Imaging of amyloid beta in Alzheimer's disease with 18F-BAY94-9172, a novel PET tracer: Proof of mechanism. *Lancet Neurology*, 7(2): 129–135, 2008.

Rowe CC, Ng S, Ackermann U, Gong SJ, Pike K, Savage G, et al. Imaging beta-amyloid burden in aging and dementia. *Neurology*, 68(20): 1718–1725, 2007.

Salmon E, Garraux G, Delbeuck X, Collette F, Kalbe E, Zuendorf G, et al. Predominant ventromedial frontopolar metabolic impairment in frontotemporal dementia. *NeuroImage*, 20(1): 435–440, 2003.

Salmon E, Kerrouche N, Herholz K, Perani D, Holthoff V, Beuthien-Baumann B, et al. Decomposition of metabolic brain clusters in the frontal variant of frontotemporal dementia. *NeuroImage*, 30(3): 871–878, 2006.

Sampathu DM, Neumann M, Kwong LK, Chou TT, Micsenyi M, Truax A, et al. Pathological heterogeneity of frontotemporal lobar degeneration with ubiquitin-positive inclusions delineated by ubiquitin immunohistochemistry and novel monoclonal antibodies. *American Journal of Pathology*, 169(4): 1343–1352, 2006.

Sanchez-Valle R, Forman MS, Miller BL, and Gorno-Tempini ML. From progressive nonfluent aphasia to corticobasal syndrome: A case report of corticobasal degeneration. *Neurocase*, 12(6): 355–359, 2006.

Seelaar H, Klijnsma KY, de Koning I, van der Lugt A, Chiu WZ, Azmani A, et al. Frequency of ubiquitin and FUS-positive, TDP-43-negative frontotemporal lobar degeneration. *Journal of Neurology*, 257(5): 747–753, 2010.

Seeley WW, Crawford R, Rascovsky K, Kramer JH, Weiner M, Miller BL, et al. Frontal paralimbic network atrophy in very mild behavioral variant frontotemporal dementia. *Archives of Neurology*, 65(2): 249–255, 2008.

Seeley WW, Menon V, Schatzberg AF, Keller J, Glover GH, Kenna H, et al. Dissociable intrinsic connectivity networks for salience processing and executive control. *The Journal of Neuroscience*, 27(9): 2349–2356, 2007.

Shimizu H, Hokoishi K, Fukuhara R, Komori K, and Ikeda M. Two cases of frontotemporal dementia with predominant temporal lobe atrophy. *Psychogeriatrics*, 9(4): 204–207, 2009.

Sjogren M, Gustafson L, Wikkelso C, and Wallin A. Frontotemporal dementia can be distinguished from Alzheimer's disease and subcortical white matter

dementia by an anterior-to-posterior rCBF-SPET ratio. *Dementia and Geriatric Cognitive Disorders*, 11(5): 275–285, 2000.

Sonty SP, Mesulam MM, Thompson CK, Johnson NA, Weintraub S, Parrish TB, et al. Primary progressive aphasia: PPA and the language network. *Annals of Neurology*, 53(1): 35–49, 2003.

Sonty SP, Mesulam MM, Weintraub S, Johnson NA, Parrish TB, and Gitelman DR. Altered effective connectivity within the language network in primary progressive aphasia. *The Journal of Neuroscience*, 27(6): 1334–1345, 2007.

Thompson PM, Hayashi KM, Dutton RA, Chiang MC, Leow AD, Sowell ER, et al. Tracking Alzheimer's disease. *Annals of the New York Academy of Sciences*, 1097: 183–214, 2007.

van de Pol LA, Hensel A, Barkhof F, Gertz HJ, Scheltens P, and van der Flier WM. Hippocampal atrophy in Alzheimer disease: Age matters. *Neurology*, 66(2): 236–238, 2006a.

van de Pol LA, Hensel A, van der Flier WM, Visser PJ, Pijnenburg YA, Barkhof F, et al. Hippocampal atrophy on MRI in frontotemporal lobar degeneration and Alzheimer's disease. *Journal of Neurology, Neurosurgery & Psychiatry*, 77(4): 439–442, 2006b.

Varma AR, Adams W, Lloyd JJ, Carson KJ, Snowden JS, Testa HJ, et al. Diagnostic patterns of regional atrophy on MRI and regional cerebral blood flow change on SPECT in young onset patients with Alzheimer's disease, frontotemporal dementia and vascular dementia. *Acta Neurologica Scandinavica*, 105(4): 261–269, 2002.

Vemuri P, Simon G, Kantarci K, Whitwell JL, Senjem ML, Przybelski SA, et al. Antemortem differential diagnosis of dementia pathology using structural MRI: Differential-STAND. *NeuroImage*, 55(2): 522–531, 2011.

Whitwell JL, Anderson VM, Scahill RI, Rossor MN, and Fox NC. Longitudinal patterns of regional change on volumetric MRI in frontotemporal lobar degeneration. *Dementia and Geriatric Cognitive Disorders*, 17(4): 307–310, 2004a.

Whitwell JL, Avula R, Senjem ML, Kantarci K, Weigand SD, Samikoglu A, et al. Gray and white matter water diffusion in the syndromic variants of frontotemporal dementia. *Neurology*, 74(16): 1279–1287, 2011.

Whitwell JL, Jack Jr CR, Pankratz VS, Parisi JE, Knopman DS, Boeve BF, et al. Rates of brain atrophy over time in autopsy-proven frontotemporal dementia and Alzheimer disease. *NeuroImage*, 39(3): 1034–1040, 2008.

Whitwell JL, Jack Jr CR, Parisi JE, Knopman DS, Boeve BF, Petersen RC, et al. Rates of cerebral atrophy differ in different degenerative pathologies. *Brain*, 130(Pt 4): 1148–1158, 2007a.

Whitwell JL, Jack Jr CR, Parisi JE, Senjem ML, Knopman DS, Boeve BF, et al. Does TDP-43 type confer a distinct pattern of atrophy in frontotemporal lobar degeneration? *Neurology*, 75(24): 2212–2220, 2010.

Whitwell JL, Josephs KA, Rossor MN, Stevens JM, Revesz T, Holton JL, et al. Magnetic resonance imaging signatures of tissue pathology in frontotemporal dementia. *Archives of Neurology*, 62(9): 1402–1408, 2005.

Whitwell JL, Przybelski SA, Weigand SD, Ivnik RJ, Vemuri P, Gunter JL, et al. Distinct anatomical subtypes of the behavioural variant of frontotemporal dementia: A cluster analysis study. *Brain*, 132(Pt 11): 2932–2946, 2009.

Whitwell JL, Sampson EL, Loy CT, Warren JE, Rossor MN, Fox NC, et al. VBM signatures of abnormal eating behaviours in frontotemporal lobar degeneration. *NeuroImage*, 35(1): 207–213, 2007b.

Whitwell JL, Warren JD, Josephs KA, Godbolt AK, Revesz T, Fox NC, et al. Voxel-based morphometry in tau-positive and tau-negative frontotemporal lobar degenerations. *Neurodegenerative Diseases*, 1(4–5): 225–230, 2004b.

Williams GB, Nestor PJ, and Hodges JR. Neural correlates of semantic and behavioural deficits in frontotemporal dementia. *NeuroImage*, 24(4): 1042–1051, 2005.

Wilson SM, Brambati SM, Henry RG, Handwerker DA, Agosta F, Miller BL, et al. The neural basis of surface dyslexia in semantic dementia. *Brain*, 132(Pt 1): 71–86, 2009a.

Wilson SM, Dronkers NF, Ogar JM, Jang J, Growdon ME, Agosta F, et al. Neural correlates of syntactic processing in the nonfluent variant of primary progressive aphasia. *The Journal of Neuroscience*, 30(50): 16845–16854, 2010.

Wilson SM, Ogar JM, Laluz V, Growdon M, Jang J, Glenn S, et al. Automated MRI-based classification of primary progressive aphasia variants. *NeuroImage*, 47(4): 1558–1567, 2009b.

Womack KB, Diaz-Arrastia R, Aizenstein HJ, Arnold SE, Barbas NR, Boeve BF, et al. Temporoparietal hypometabolism in frontotemporal lobar degeneration and associated imaging diagnostic errors. *Archives of Neurology*, 68(3): 329–337, 2011.

Woolley JD, Gorno-Tempini ML, Seeley WW, Rankin K, Lee SS, Matthews BR, et al. Binge eating is associated with right orbitofrontal-insular-striatal atrophy in frontotemporal dementia. *Neurology*, 69(14): 1424–1433, 2007.

Zahn R, Buechert M, Overmans J, Talazko J, Specht K, Ko CW, et al. Mapping of temporal and parietal cortex in progressive nonfluent aphasia and Alzheimer's disease using chemical shift imaging, voxel-based morphometry and positron emission tomography. *Psychiatry Research*, 140(2): 115–131, 2005.

Zamboni G, Huey ED, Krueger F, Nichelli PF, and Grafman J. Apathy and disinhibition in frontotemporal dementia: Insights into their neural correlates. *Neurology*, 71(10): 736–742, 2008.

Zhang Y, Schuff N, Du AT, Rosen HJ, Kramer JH, Gorno-Tempini ML, et al. White matter damage in frontotemporal dementia and Alzheimer's disease measured by diffusion MRI. *Brain*, 132(Pt 9): 2579–2592, 2009.

Zhou J, Greicius MD, Gennatas ED, Growdon ME, Jang JY, Rabinovici GD, et al. Divergent network connectivity changes in behavioural variant frontotemporal dementia and Alzheimer's disease. *Brain*, 133(Pt 5): 1352–1367, 2010.